NASA/CR—2017-219712/SUPPL

Point-Focus Concentration Compact Telescoping Array

EESP Option 1 Phase Final Report for Public Release

Michael E. McEachen, Patrick Haynes, Christopher Peterson,
Wyatt Rodgers, Jim Spink, and Mike Eskenazi
Orbital ATK, Goleta, California

Mark O'Neill
Mark O'Neill, LLC, Fort Worth, Texas

Paul Sharps
SolAero Technologies Corp., Albuquerque, New Mexico

December 2019

NASA STI Program . . . in Profile

Since its founding, NASA has been dedicated to the advancement of aeronautics and space science. The NASA Scientific and Technical Information (STI) Program plays a key part in helping NASA maintain this important role.

The NASA STI Program operates under the auspices of the Agency Chief Information Officer. It collects, organizes, provides for archiving, and disseminates NASA's STI. The NASA STI Program provides access to the NASA Technical Report Server—Registered (NTRS Reg) and NASA Technical Report Server—Public (NTRS) thus providing one of the largest collections of aeronautical and space science STI in the world. Results are published in both non-NASA channels and by NASA in the NASA STI Report Series, which includes the following report types:

- TECHNICAL PUBLICATION. Reports of completed research or a major significant phase of research that present the results of NASA programs and include extensive data or theoretical analysis. Includes compilations of significant scientific and technical data and information deemed to be of continuing reference value. NASA counter-part of peer-reviewed formal professional papers, but has less stringent limitations on manuscript length and extent of graphic presentations.

- TECHNICAL MEMORANDUM. Scientific and technical findings that are preliminary or of specialized interest, e.g., "quick-release" reports, working papers, and bibliographies that contain minimal annotation. Does not contain extensive analysis.

- CONTRACTOR REPORT. Scientific and technical findings by NASA-sponsored contractors and grantees.

- CONFERENCE PUBLICATION. Collected papers from scientific and technical conferences, symposia, seminars, or other meetings sponsored or co-sponsored by NASA.

- SPECIAL PUBLICATION. Scientific, technical, or historical information from NASA programs, projects, and missions, often concerned with subjects having substantial public interest.

- TECHNICAL TRANSLATION. English-language translations of foreign scientific and technical material pertinent to NASA's mission.

For more information about the NASA STI program, see the following:

- Access the NASA STI program home page at http://www.sti.nasa.gov

- E-mail your question to help@sti.nasa.gov

- Fax your question to the NASA STI Information Desk at 757-864-6500

- Telephone the NASA STI Information Desk at 757-864-9658

- Write to:
  NASA STI Program
  Mail Stop 148
  NASA Langley Research Center
  Hampton, VA 23681-2199

NASA/CR—2017-219712/SUPPL

Point-Focus Concentration Compact Telescoping Array

EESP Option 1 Phase Final Report for Public Release

Michael E. McEachen, Patrick Haynes, Christopher Peterson,
Wyatt Rodgers, Jim Spink, and Mike Eskenazi
Orbital ATK, Goleta, California

Mark O'Neill
Mark O'Neill, LLC, Fort Worth, Texas

Paul Sharps
SolAero Technologies Corp., Albuquerque, New Mexico

Prepared under Contract NNC16CA23C

National Aeronautics and
Space Administration

Glenn Research Center
Cleveland, Ohio 44135

December 2019

Acknowledgments

The authors would like to thank the NASA Game Changing Development Extreme Environment Solar Power (EESP) team at Glenn Research Center, especially Fred Elliott, Jeremiah (Jay) McNatt, Annamaria Pal, and Michael Piszczor, for their insights, understanding, and encouragement.

Available from

NASA STI Program
Mail Stop 148
NASA Langley Research Center
Hampton, VA 23681-2199

National Technical Information Service
5285 Port Royal Road
Springfield, VA 22161
703-605-6000

This report is available in electronic form at http://www.sti.nasa.gov/ and http://ntrs.nasa.gov/

Point-Focus Concentration Compact Telescoping Array
EESP Option 1 Phase Final Report for Public Release

Michael E. McEachen, Patrick Haynes, Christopher Peterson
Wyatt Rodgers, Jim Spink, and Mike Eskenazi
Orbital ATK
Goleta, California 93117

Mark O'Neill
Mark O'Neill, LLC.
Fort Worth, Texas 76244

Paul Sharps
SolAero Technology Corp.
Albuquerque, New Mexico 87123

Abstract

Orbital ATK, in partnership with Mark O'Neill LLC (MOLLC) and SolAero Technologies Corp., has developed a novel solar array platform, PFC-CTA, which provides a significant advance in performance and cost reduction compared to all currently available space solar systems. "PFC" refers to the Point Focus Concentration of light provided by MOLLC's thin, flat Fresnel optics. These lenses focus light to a point of approximately 100 times the intensity of the ambient light, onto a solar cell of approximately 1/25th the size of the lens. "CTA" stands for Compact Telescoping Array[1], which is the solar array blanket structural platform originally devised by NASA and currently being advanced by Orbital ATK and partners under NASA and AFRL funding to a projected TRL 5+ by late-2018.

The NASA Game Changing Development Extreme Environment Solar Power (EESP) Option 1 Phase study has enabled Orbital ATK to generate and refine component designs, perform component level and system performance analyses, and test prototype hardware of the key elements of PFC-CTA, and increased the TRL of PFC-specific technology elements to TRL ~5. Key performance metrics currently projected are as follows: Scalability from < 5 kW to >300 kW per wing (AM0); Specific Power > 250 W/kg (BoL, AM0); Stowage Efficiency > 60 kW/m^3; 5:1 margin on pointing tolerance vs. capability; >50% launched cost savings; Wide range of operability between Venus and Saturn by active and/or passive thermal management.

Acronyms & Abbreviations

AD	Angstrom Designs, Inc.
AU	Astronomical Unit
BoL	Beginning of Life
CGF	Composite Grid Frames
CLM	Concentrator Lens Modules
CPM	Concentrator Power Modules
CTA	Compact Telescoping Array
CTE	Coefficient of Thermal Expansion
EESP	Extreme Environment Solar Power
EoL	End of Life
GCR	Geometrical Concentration Ratio
ISS	International Space Station
LILT	Low Intensity, Low Temperature

MOLLC	Mark O'Neill, LLC
NFL	Nominal Focal Length
OA	Orbital ATK
OCR	Optical Concentration Ratio
PFC	Point Focus Concentrator
PV	Photovoltaics
SEP	Solar Electric Propulsion
TRL	Technology Readiness Level

Introduction

For decades now, NASA and others have been investing in technologies to enable affordable, reliable exploration of the most inhospitable reaches of our solar system. One of the technologies to enable this goal is solar-powered electric propulsion (SEP)[2], primarily for its extremely high specific impulse. The challenge however is how to efficiently generate adequate power where the sunlight is much dimmer, down to as low as 1% of the intensity at Earth orbit. Without enhancements such as optical concentration or special solar cell screening, deep space conditions result in solar cells operating too cold and with too little current and voltage to effectively produce power. The surface area required to gather enough light energy grows to unreasonable sizes, and the cost and mass increase, especially given the radiation shielding that must be applied over the active photovoltaics for missions near Jupiter and Saturn. Optical concentration promises to address all these challenges, with the additional benefit of lowering system cost.

Along many fronts, but most intensively under the subject NASA EESP-Game-Changing Technology program Option I Phase which this report reviews, Orbital ATK and its partners have been rapidly developing the constituent elements required to make our Point Focus Concentrator (PFC) Compact Telescoping Array (CTA) system ready for near-term mission infusion.

CTA: Optimal System Architecture for Efficiency and Accuracy

Due to the high optical concentration ratio (OCR) employed by PFC, the alignment between lenses and PV collectors must be maintained within a limited tolerance window, depending on the chosen geometrical concentration ratio (GCR). Precise alignment is achievable with the unique attributes of the Compact Telescoping Array (CTA) architecture, which is a lightweight, compactly stowed and automatically deployable structural platform for blanket array deployment and support. The basic idea for CTA was originally proposed by NASA[3], and CTA has been rapidly advanced by two Phase-II SBIRs led by Angstrom Designs, Inc., with Orbital ATK as partner. A full listing of programs actively developing and/or leveraging CTA is provided in Table 12. CTA comprises tensioned photovoltaic (PV) blankets supported by a central truss mast, a configuration reminiscent of the iconic solar arrays on the International Space Station (ISS). Indeed, this architecture has been demonstrated[4] to provide the most efficient known means of deploying and supporting a planar blanket array, given typical spacecraft structural and packaging requirements, and it is an ideal platform for PFC lens and receiver blankets as well. Extremely high values achieved for key efficiency metrics by the CTA platform (deployed blanket area per system mass & volume and high deployed stiffness & strength) also contribute to the enabling performance achieved with PFC blankets and optical concentration. An overview of the PFC-CTA system is shown in Figure 1. The comparative suitability for PFC on CTA vs. Orbital ATK's UltraFlex platform is presented in Table 1.

Table 1. CTA vs. UltraFlex Compatibility with PFC

Criterion	CTA	UltraFlex
Compatible with large, repeating blanket modules (SPM's)	**Yes,** rectangular blankets are ideal for modular assembly with simple attachment to blanket tension elements (tapes)	**No**, triangular "gores" must be divided into multiple sized "gorelets" which are not interchangeable.
System level planarity defined by discrete, precisely located points	**Yes,** long axis of wing is defined by accurately located blanket tape terminations supported by the central truss. Flatness in the long axis is guaranteed by tension.	**No**, blankets are supported continuously along each edge by radial spars; spar bending or misalignment at hub will produce significant distortion of blanket flatness.
System pointing obtained by a large diameter, structurally optimal lattice truss	**Yes,** central truss is a high-precision pointing structure, ideally suited for achieving extremely tight positional repeatability and thermal stability	**No**, relatively shallow beam section, monolithic radial spars provide structure. Spar beam stiffness (EI) is approximately 1/20th that of CTA's central truss.
Stowed and deployed conditions compatible with parallel, precisely positioned blankets	**Yes,** lens blanket z-folded, inter-leaved with PV blanket; Lens focal length standoff provided by separation between tape attachments on blanket panels.	**No,** obtaining required lens standoff would entail additional structure as spars are much less tall than lens focal length.

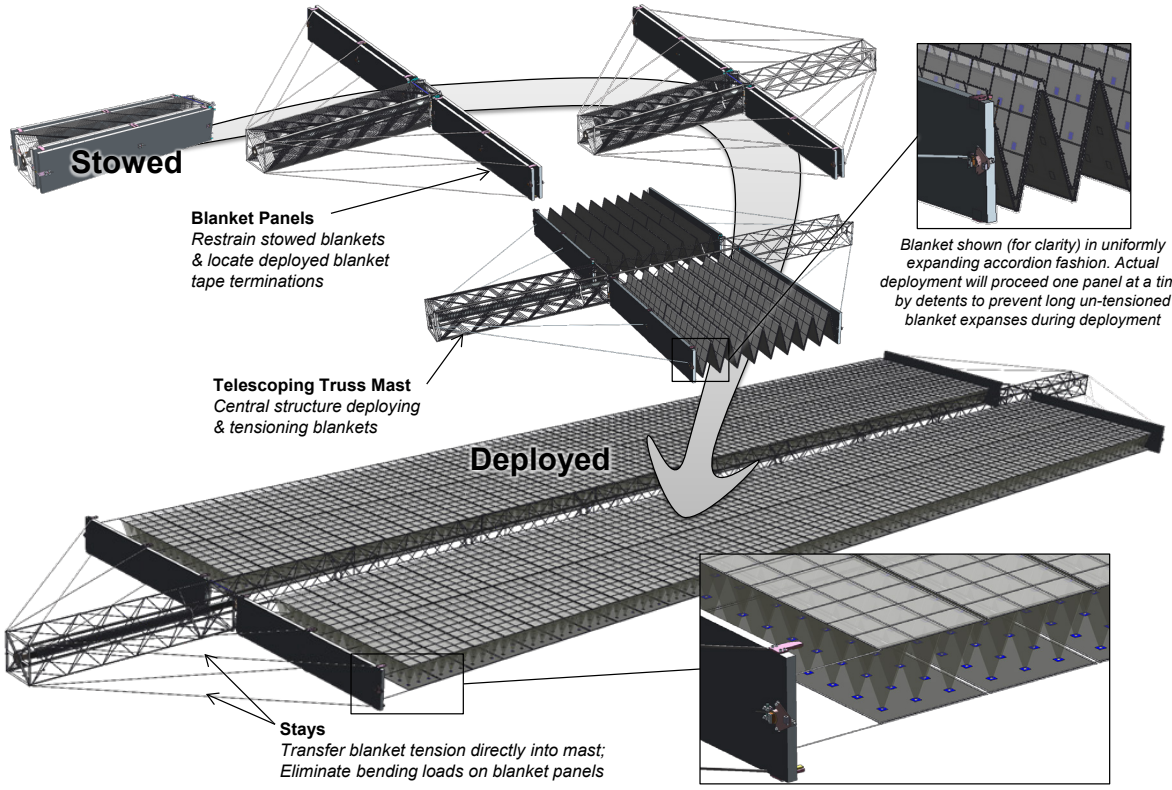

Figure 1. PFC-CTA System Overview

The ISS masts, built by Orbital ATK (then known as AEC-Able Engineering), were constructed of aluminum and stainless steel aircraft cable, and require a substantial canister for stowed containment and mast deployment. CTA, in contrast, comprises a lattice truss of unidirectional high-modulus carbon fiber (nearly 6x the specific stiffness of aluminum), and deployment of the CTA wing is accomplished by a single motorized lead screw which pulls the nested mast segments out from their stowed positions into their deployed, precisely latched, positions.

A second key difference between CTA and the ISS arrays is that the CTA blanket panels are not subjected to bending loads from tensioning the blankets. Thanks to the segmented, telescoping mast construction, the mast is able to extend beyond the blanket length. This enables the use of tension-carrying elements ("stays") running between the blanket tapes and the mast ends. Eliminating bending loads from the blanket panels saves significant mass and volume, since the blanket panels no longer require a deep beam section. A secondary function of the telescoping mast extending beyond the blanket length is to provide clearance between the blanket and electric propulsion plume, and to avoid shadowing of the blanket by the spacecraft. While CTA blanket panels are of similar honeycomb sandwich construction as typically employed for conventional planar solar arrays, for CTA, the total panel area required is on the order of 3% of the blanket area, vs. 100% for a planar array. Finally, on a related note, the blanket panels fold to stow alongside the mast root segment, providing a compact rectangular stowed volume, which is much easier to package alongside the spacecraft bus than the "T" stowed configuration posed by the ISS (and many other tensioned blanket arrays).

The thermal stability and precision deployment provided by CTA's open lattice, carbon fiber construction, deployed with a bare minimum of joints and latches, are truly enabling for PFC's alignment performance. The only source of mast deployment position repeatability error is from the latches at the root of each moving segment, so these latches incorporate high-precision, self-preloading features, which practically eliminate deployed positional uncertainty, and provide a stiff, determinate joint between deployed mast segments. The effects of these latches on pointing, as well as bending of the mast due to thermal expansion, have been included in pointing budgets and margins developed under the subject EESP study.

CTA's use of tensioned blankets is beneficial to PFC in virtually eliminating the possibility of bending or bowing in the blanket long axis. Additionally, having the blanket supported only at the root and the tip of the mast, reduces the maximum off-pointing of the blanket by 50% compared with a blanket that is attached continuously along the mast length. CTA's use of discrete tension tapes between the base and tip panels also facilitates a key feature of PFC on CTA: the ability to easily adjust the focus of the lenses vs. the PV for **robust thermal management** at near-sun orbits, discussed below.

Another key innovation employed by PFC-CTA is the use of composite grid frames (CGF) on the lens and PV blankets. The grid frames provide the structure needed to keep each blanket flat despite being tensioned with a limited number of tapes. The thin, near-zero-CTE grid frames maintain flatness between tape constraints, a span of approximately 1 m. Blanket crosswise bow, bending or distortion of the blanket surface between blanket tension tapes, has been estimated based on CGF front-to-backside thermal gradients calculated by detailed 3-D thermal modeling, and actually contributes only a trivial amount of misalignment relevant to the pointing budget.

These frames are very effective in enabling low-cost manufacturing of modular CPMs and CLMs (Concentrator Power Modules and Concentrator Lens Modules) and are also a simple and effective method to manage the vibration loading that the stowed blanket is subjected to during launch. For in-plane loads, the composite strips manage compressive loads between distributed masses in a blanket out to the blanket outer edges, where they are snubbed by constraints located periodically on the blanket panels. For out-of-plane loads, the grid strips stack directly on grid strips of adjacent CPMs and/or CLMs, providing a stiff load path, and since the grid spacing is relatively frequent, there are no large spans of unsupported lens or PV/radiator area, ensuring high stowed resonance modes and correspondingly low stresses and dynamic amplitudes in these components.

Both the Lens Blanket and Cell Blanket are assembled by fastening the modular CGF subassemblies to the longitudinal blanket tapes. The baseline blanket tape material is carbon fiber, the same material used for the mast construction. Matching the CTE between mast and blanket minimizes the stroke required of blanket tensioning springs (reducing mass and volume of these simple mechanisms). The low CTE also minimizes the in-plane displacement between the lens and PV blankets. In this Option 1 phase, the blanket tape design details have been developed, validating key performance characteristics: robustness to folding for stowage, load management (strength) without creep, and required end terminations.

EESP Option 1 Phase Study Tasks and Results

Orbital ATK (OA) developed and followed a Work Breakdown Schedule (WBS) for the subject EESP study which was structured to mitigate the key risks associated with advancing the PFC system in preparation for space flight operation. The Base Phase activity provided the ideal conditions for rapidly and cost-effectively mitigating these risks, preparing the technology for the high fidelity, detailed design, analysis and testing to be performed in the two optional follow-on EESP study phases. This work was roughly divided into two categories: hardware development/testing and system analysis. This combination provided the ability to incorporate lessons learned from prototype hardware build and test experiences and was a key to identifying and validating baseline materials, dimensions, assembly techniques, function and performance.

Table 2 is a summary of the PFC Risk Matrix, followed by a narrative description of the understanding of each risk, and the EESP study activities performed to mitigate each risk.

Table 2. PFC Risk Matrix for Proto-Flight Program Starting Now

I.D.	Risk Statement	Risk Context	L	Likelihood Rationale	C	Consequence Rationale	L·C	Timeframe	Option 1 Final Update
1	Given that PFC lenses are newly developed, there is a possibility that the lenses will be too expensive to be practical for adoption	PFC lenses must be significantly less costly than the active PV associated with an un-concentrated system to be competitive	3	Successful production of all lens construction variants has been demonstrated to date; scale-up plans appear credible	3	Lenses are simple components, made from commercially-available materials, and have been successfully produced at prototype quantities	9	End of Option 2 (which focuses on production scale-up)	Titanium mesh reinforced and CMG (glass) lenses were successfully produced for Option 1 prototype, including process refinements to optimize yield.
2	Given that there is a limited pointing tolerance for a PFC solar array, there is a possibility that additional features are required to ensure that lenses maintain acceptable optical alignment with PV cells throughout mission	High (>10X) concentration PV for spacecraft has historically suffered from the challenge of ensuring initial (build, 0-g deployed) and operational (thermal distortion, structural dynamics) alignment	2	Rapid progress with telescoping mast and high-precision latches have substantially mitigated the likelihood of this risk. Additional hardware built & tested will further mitigate this risk in the near term.	3	If further refinement of pointing estimates indicate lack of pointing margin, additional stability features (thermal control) would increase complexity and system cost.	6	End of Option 2 (primarily mitigated by work on other programs)	CTA SBIR Activities and other Flight telescoping boom programs have rapidly advanced design and analytical maturity of CTA platform. Pointing accuracy much tighter than needed for PFC has been demonstrated on similar systems.
3	Given that the solar cells are subjected to many suns of light, there is the possibility that the cells will over-heat and be damaged	Refined thermal analysis performed on cells optimized for high-concentration operation indicates that cells operate at acceptable temperatures	2	Refined designs and analysis developed over the course of EESP have driven this risk continually downwards	3	If CPV cells are shown by refined testing to be less effective than currently thought, defocusing or other heat management may be needed.	6	Option 1	4J IMM cells with ceramic heat spreader (design derived from terrestrial CPV built for 1600 suns) and radiator have been built in Option 1, with thermal analysis indicating tolerable temps at Venus intensity. Option to defocus blankets for less thermally efficient PV is viable.
4	Given that stowed PFC lens blanket has not been tested, there is the possibility that a PFC blanket requires redesign to prevent damage by stowage and/or dynamic (vibration) environments	Flat-packed lens frame blanket is a relatively novel configuration and needs to be validated. Thin lenses folded into compact stack could potentially tear or stick together.	2	Brassboard models of PFC grids and mesh-reinforced lenses indicate that they will be robust. Further testing (vibe) will mitigate residual risk.	3	If vibration testing indicates fragility, design changes may be needed increasing cost, mass and volume.	6	Option 1	Blanket-level vibration and deployment testing of stacked PV and lens modules has demonstrated viability of both metallic mesh and glass superstrate lenses.
5	Given that they have not yet been flown, there is the possibility that PFC lenses and/or PV cells will not survive deployed environments	CPV arrays have suffered on-orbit failures due to unforeseen issues. PFC designs seek to leverage lessons learned, but new designs always bring uncertainty.	2	Multiple lens/ mounting combinations were built and tested during Option 1	3	If none of the several configurations developed in Option 1 succeed, a baseline configuration will be further delayed	6	Option 1	New, low-stress lens mounting designs address lessons learned in Base Phase. New "symmetric pultrusion laminate" CGF design mitigates bow instability.

Risk I.D. 1: "Given that PFC lenses are newly developed, there is a possibility that these lenses (lens arrays) will be more expensive to produce than expected"

This risk encompasses the basic technical feasibility of building flat Fresnel lens arrays suitable for space flight, and the economics of the constituent materials and processes. To address this question, a number of prototype lenses were produced by Orbital ATK's PFC team member Mark O'Neill, LLC (MOLLC) at the outset of the Study and assembled into developmental composite grid frames. A significant advance in the lens technology since the Base Phase is that these lenses were built using point-focus tooling, developed by MOLLC under a SBIR Phase IIE program.

The brassboard lens samples were produced on disposable plastic tooling, which itself is produced in a roll-to-roll process, capable of producing 10 MW of tooling in a matter of days. The plastic tools are compact and can be efficiently stacked and/or arrayed for dispensing of the silicone, addition of the reinforcing mesh, and for curing. The silicone for the brassboard lenses was manually mixed and spread, whereas a production run would employ mix-meter-dispense equipment, which is well-established in the silicone plastics production industry – medical supplies, for example. Another difference between the prototype and "flight" is that these lenses were made from medical-grade, not space-grade silicone. The two grades of silicone are believed to be chemically identical, but the medical grade silicone is less expensive. These adjustments and compromises were justified based on the high initial costs associated with making a small prototype quantity for this study. These initial costs relate primarily to tooling and/or minimum buy requirements, costs that are well known and therefore do not pose actual "risk" to a future flight program.

The initial effort in building the Option 1 prototype lenses included process refinement experiments aimed at producing mesh reinforced lenses that have an optimal base thickness. The experiments resulted in a process that produces an optimal base thickness, which is just thicker than the mesh, and was tailored for making both metallic mesh and fiberglass mesh lenses.

MOLLC produced 5 prototype lenses in each of the following configurations: Titanium mesh, stainless steel mesh, fiberglass mesh, and with glass superstrate (no mesh). These configurations represented the full range of options under consideration at the start of the Base Phase. Although initially favored due to their inexpensive producibility, stainless steel mesh is no longer being pursued, as it is higher mass, lower strength, and higher CTE than the similarly-producible titanium mesh. Glass fibers are also no longer being actively pursued, as they require a mounting scheme more complicated than the corner fasteners on the metallic mesh lenses, and the glass fibers are unable to react to the high compressive forces applied by the high-CTE silicone at the cold operating temperatures. This condition results in a large amplitude of radial motion at the lens corners, on the order of 1 mm, compared to the 0.1 mm radial motion associated with the titanium mesh lenses. Examples of the prototype lenses produced by MOLLC during Option 1, and their associated light spots, are shown in Figure 3.

An additional quantity of prototype lenses were also given a UV-rejection coating, intended to block the UV wavelengths that have been shown to damage silicone at high doses. This coating is also intended to reduce the tackiness characteristic of silicone, and to reduce light wasted by reflection. While the UV blocking characteristic of this coating was demonstrated on the fused silica witness sample that was produced at the same time as the lenses (see Figure 2), the coated lenses unfortunately did not benefit from the loss of "tackiness" as expected. Process refinements were identified by MOLLC and the coating vendor, and it is expected that another lot of lenses would not suffer this defect.

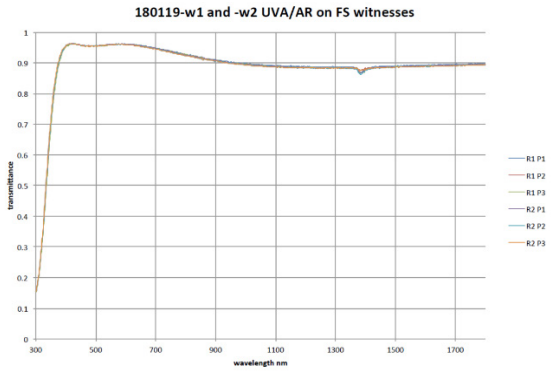

Figure 2. UVR Coating Transmittance

Figure 3. Prototype Lenses

Another contributing factor in Risk ID 1 (lens array affordability) relates to the composite frame used to support the lenses. The frames themselves must be affordable to produce, the assembly of the lenses into the frames must be manageable, and the lenses and/or lens modules must be individually replaceable in the event of damage, e.g., due to a handling mishap.

During the Base Phase, Composite Lens Frames were produced using individual carbon fiber sticks, with the lenses assembled integrally in a sandwich construction. This method was favored as it provides the most determinate mounting for the lenses, ensuring alignment and flatness. However, this construction method has at least two severe drawbacks. For one, the lenses were not serviceable in any way once the grid module was assembled. This would mean the scrapping of an entire module if a lens were to be damaged. Additionally, and more significantly, this perimeter, “sandwich” mounting resulted in unacceptably high stresses in both the lens mesh and also in the composite grid, Figure 4.

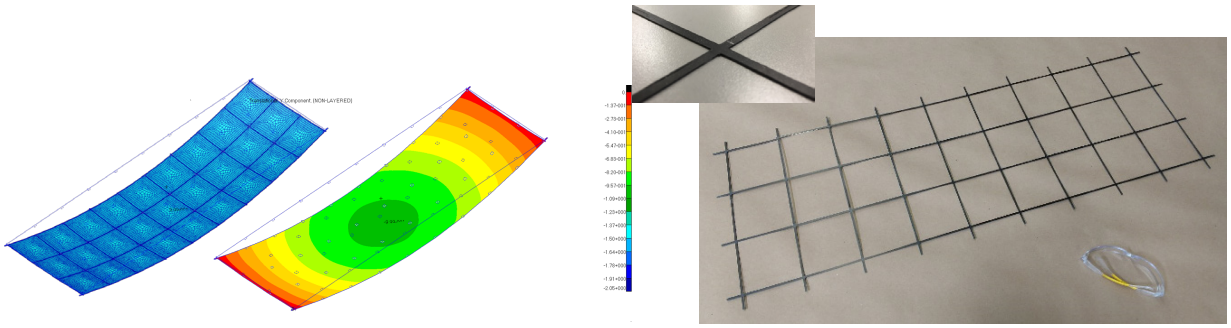

Figure 4. Molded CGF, FEA & Prototype

The first task in Option 1 was to identify a lens mounting scheme to overcome these issues. This was a challenging task, and, as is characteristic of many development programs, resulted in navigating a few blind alleys. Initially, there was an attempt to “surface-mount” the lenses over a molded composite grid frame. This would have eliminated the process of assembling a grid frame from individual carbon sticks, while allowing the lenses to be individually removable. Several prototype iterations were produced, but the molded composite assembly had the inevitable condition wherein the grid intersections possessed twice as much fiber as the straight sections. This caused the finished frames to be much weaker at these intersections (due to the low resin content) and also the frames were not nearly as flat as those made with individual sticks. The molded frames also posed a challenge of how to flush-mount a lens without adding thickness or introducing snagging hazards to the assembly deployment. Finally, finite element modeling of the surface-mounted lens demonstrated that the thru-thickness asymmetry of the assembly could result in a significant (approximately 25 mm) thermally-induced bow across the length of each lens module, unless the lenses were completely mechanically decoupled from the frame, which was considered infeasible. This bow would have caused unacceptable pointing errors and misalignments in the deployed system.

Although the molded grid frame approach was ultimately abandoned, the lessons learned helped to guide the next design iteration. The benefits of “brick-laid” stick construction were confirmed: a symmetric construction, continuous and uniform fibers across the long span, and the addition of lens mounting features, located ideally at the lens corners, and at the neutral axis (mid-plane) of the lens module vs. out-of-plane bending all contributed to a successful new design: building the grid frame as an assembly of continuous sticks in the long axis, sandwiching “gusset” plates at the intersection points, and reducing the grid density such that there are short, three-lens-wide spans of lens sub-strings without vertical sticks. Only the top and bottom sticks contribute to out-of-plane bending stability and stiffness, while the remaining, interior sticks serving as lightly-loaded mounting points for the lens corners, and reacting in-plane stowed launch/ vibration loads. The gusset plates are made to closely match the low CTE of the carbon sticks, and therefore to offer the least thermally induced mechanical strains on the bonds to the sticks.

Orbital ATK built several prototype brassboard lens grid assemblies, refining the process for adhesive application, arrangement of the sticks, and whether or not the individual layers of the assembly were allowed to cure separately or together. The PFC lens frame assembly is presented in Figure 5.

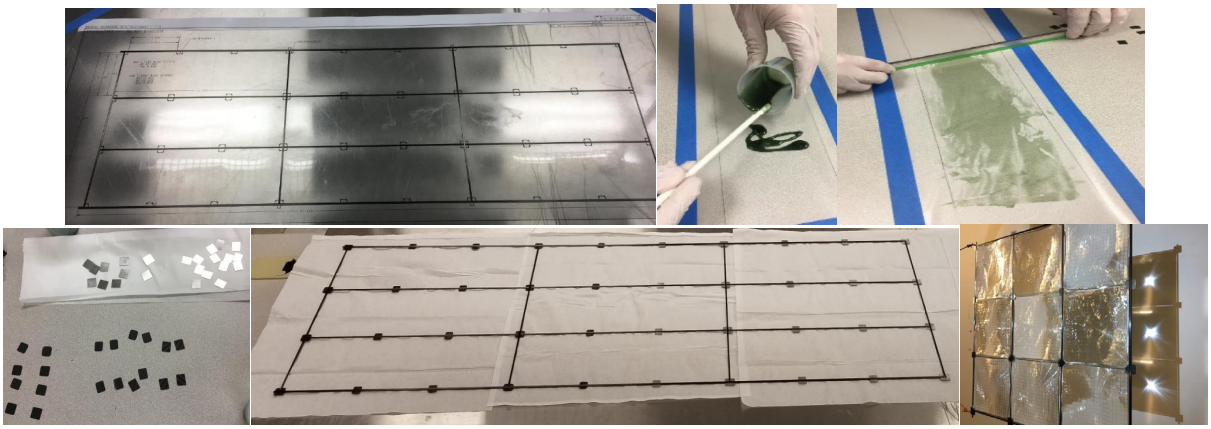

Figure 5. Lens Panel Assembly

The lessons learned in the development of the lens grid was carried over to the design of the PV grid. Similar to the lens grid, a series of high-modulus, rectangular strips (“sticks”), are arranged to provide groups of 3 adjacent PV cells. A thin composite sheet, formed in a diagonal lattice configuration is used to provide the substrate for mounting the PV cells. The CTE of the lattice and sticks are similar, resulting in low thermal stresses. The cross grid provides accurate mounting locations for the PV cells with minimal interface with the PV cell’s thermal radiators. Adhesive is used to bond the composite rods which sandwich the cross grid laminate. A template printed on Mylar ensures accurate alignment of the thin composite rods. Continuous rods are used along the long axis edge to provide max strength in the weakest bending mode. The rods on one side of the out of plane direction of the grid panel extend beyond the cross grid laminate to provide attachment points to the composite tow blanket tapes. The PV grid frame assembly is shown in Figure 6.

While the PV grids developed in Option 1 were successful and viewed as a viable baseline for future implementation, several improvements have been identified for the next iteration. Firstly, the process of assembling the cross grid laminate and composite rods with adhesive is tedious and time consuming. A tooling fixture that holds the cross grid and composite rods in place during assembly would reduce labor and improve accuracy of the PV composite grid.

A second enhancement is to optimize the profiles (width and thickness) of the composite sticks. The PV grid built in Option 1 utilized off-the-shelf profiles for expedience; custom profiles are also available at reasonable cost and lead time, and would produce a more optimized frame structure. The thickness of the composite frames that constitute the PFC blankets are key drivers of stowed volumetric efficiency, and therefore must be made as thin as necessary to achieve the required structural performance.

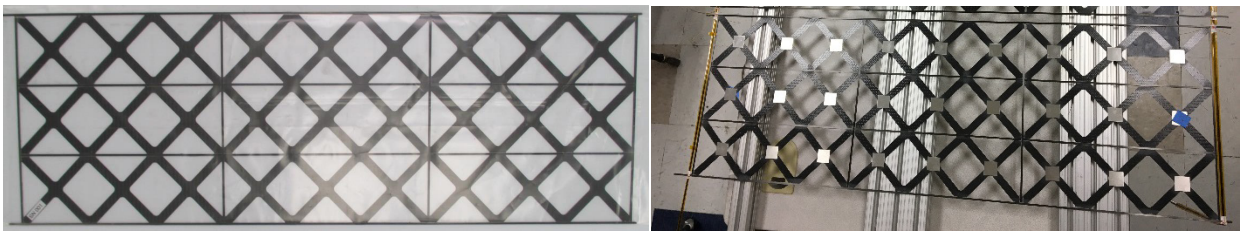

Figure 6. PV Grid Frame Assembly

It should also be noted that a key to the affordability and scalability of PFC relative to other deep space solar arrays is related to the 25X concentration factor. Photovoltaic cell production is a complicated, capital-intensive process, and LILT operation further reduces yields. The current global capacity for space photovoltaics is on the order of 1-2 MW/ year. If NASA were to pursue missions requiring high power for deep space, say a single mission requiring 500 kW, the PV production required for a “1-sun” array would pose a significant challenge to the industry (approximately ¼ of total capacity for a single mission). If this mission utilizes 25X concentration, the same 500 kW power production is achieved with only 20 kW of PV area, equivalent to merely a pair of typical commercial satellites. The significant cost benefits of high concentration on spacecraft and launch costs are considered further in and accompanying text.

Risk I.D. 2: Given that there is a limited pointing tolerance for a PFC solar array, there is a possibility that the lenses fail to maintain acceptable optical alignment with PV cells throughout mission

The risk of the lenses failing to focus light onto the collector cell is fundamental to any concentrator array, but the CTA architecture has been evaluated in detail in the course of this Study, and perhaps surprisingly, as structural and thermal models have been refined, pointing budgets have generally improved. As of the conclusion of the Base Phase Study, the maximum amount of the available pointing budget used in any degree of freedom is 20%; in other words,

the wing is expected to point 5 times more accurately than needed to keep the light spots on the solar cells. Of course the size of the cell is a variable that can be adjusted independent of the lens design, to provide a larger boundary to the focused light if needed.

A table of possible sources of misalignment was assembled, and estimates of expected inaccuracy or distortion were made for each source. Misalignments were grouped according to environmental (primarily thermal), dynamic (e.g., due to spacecraft maneuvering), and initial construction imperfections and deployment repeatability. A summary of estimated (1-sigma) misalignments are summed and compared vs. budgets and presented in Table 3. Definitions of alignment errors and primary sources are shown in Figure 7. Determination of the pointing budgets is presented in Table 4.

Table 3. Alignment Budget

lateral	axial	piston					
dx	dy	dz	rx	ry	rz	**Distortions**	Analysis reference/ Comment
(mm)			(degrees)				
						Boom Bending	
	0.04		0.1			Front vs. Backside longerons gradient	MathCAD spreadsheet with self-shadowing temp estimates
						Boom Twist	
						Gradient between crossing diagonals	nominally zero - equal light incident on crossing pairs
						Blanket distortion	
	0.84					In-plane dilation	MathCAD with front/backside gradients from TD
0.01				0.02		Crosswise bow	MathCAD with front/backside gradients from TD
						Blanket dynamic displacement	
		1				First-mode amplitude (peak-valley)	Depending on system damping and ACS impulses
0.03	0.03	0.03	0.1	0.1	0.1	**S/c ACS pointing accuracy**	WAG based on NASA ACS paper - probably conservative
						Initial Construction/ Alignment	
	0.01		0.02			Opposing wing (boom) co-alignment o	based on .005" tilt error at longeron ends
	0.01		0.02			Boom initial straightness	
0.01				0.02		Boom twist	No known source of initial pre-twist
0.5	0.5	0.5	0.01	0.01		Blanket co-alignment	Gravity shifts, backlash/clearance in joints
0.55	1.43	1.53	0.25	0.15	0.1	**TOTAL MISALIGNMENTS**	
7	7	10	2	2	2	**Total Budgets**	See separate table for Budget Determination
8%	20%	15%	12%	8%	5%	**CBE/Budget (% of budget used)**	Minimum margin is dy; could elongate lens in Y dimension
13	5	7	8	13	20	**Predicted = X times better than budget**	

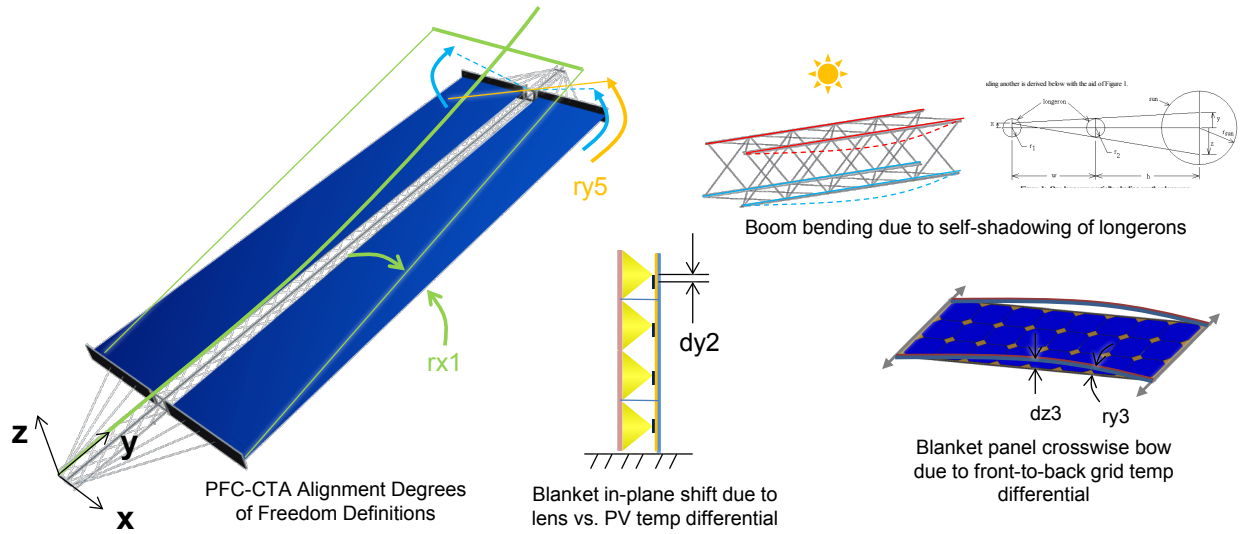

Figure 7. PFC CTA Alignment Definitions

Table 4. PFC Alignment Budget Determination

DoF	Description	Source
dx, dy	Lateral shift	PV collector is oversized vs. Lens "spot", e.g. 2 cm PV cell for 0.6 cm spot = ±0.7 cm (7 mm) tolerance
dz	Lens-Cell Focal Length	1% loss in collector efficiency for 5% error in focal length (.05*200mm = 10 mm)
rx	Lens tilt vs. Sun	Lens efficiency has no measureable drop-off at less than 2° error vs. sun line
dx, dy	Wing tilt vs. Sun	Blanket gross tilt creates a lateral shift between light spot and PV cell. 2° tilt --> 0.7 mm shift (lateral shifts due to angular errors included in rollup)

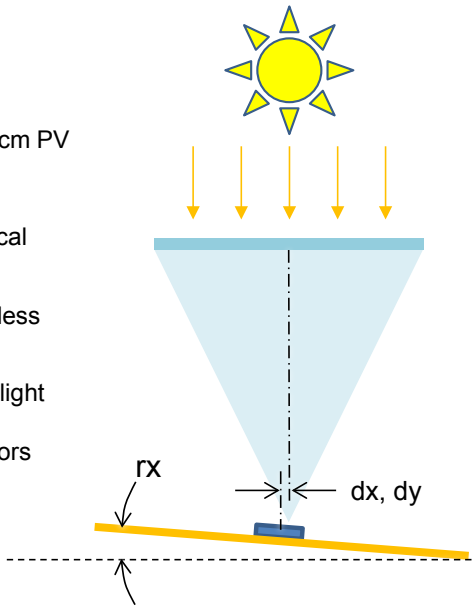

The Option 1 activity included the design and construction of a complete, truncated PFC blanket assembly. The blanket consists of 4 lens and 4 PV modules, supported by blanket tapes. This blanket subassembly provided initial indication of the ability to package and deploy a precisely aligned array of lenses and PV cells, using the methods developed during the past two study phases. Due to this robust initial pointing margin, the pointing budget was not further refined during Option1. Future PFC work would include the construction of a detailed finite element model which will be exercised to determine detailed dynamic interactions in the wing, including a jitter analysis, and dynamics coupling between the tensioned blankets and the central truss mast and blanket spreader panels.

Risk I.D. 3: Given that the solar cells are subjected to many suns of light, there is the possibility that the cells will over-heat and be damaged

Thermal management is an obvious concern with any solar concentrator, and was addressed in this Study by a combination of analysis and design features. Detailed thermal analysis of the entire blanket system was performed. All blanket components were included in a 3-D Thermal Desktop model, and subjected to a variety of lighting conditions corresponding to various planetary locations as a familiar reference point for illumination conditions that vary from 0.7 AU (Venus, ~2 suns) to 10 AU (Saturn, ~0.01 suns). The fidelity of the solar cell modeling was given special attention, given the extreme environmental influences inflicted by the 200x range in solar flux input and the consequent changes in light conversion efficiency. SolAero was consulted to review the modeling assumptions and parameters. MOLLC provided light intensity and current concentrations as filtered by the color-mixing lens into each solar cell junction, over the 2 x 2 cm cell area in a 20 x 20 grid, sufficient to resolve thermal gradients related to the focused light spot. These inputs were imported as heat inputs in the solar cell blanket thermal model, which was meshed to an equivalent grid density. The resulting temperature profiles (over the cell area) were then provided to SolAero, which performed detailed power analyses for a wide range of AUs, based on a cell gridline design optimized (somewhat arbitrarily) for operation at Mars orbit.

The lens thermal and power modeling was informative and encouraging, indicating that the thermal radiators are indeed effective (and necessary) for spreading and rejecting waste heat from the cell. Furthermore, the analysis demonstrates that a 3J cell will be unable to manage the intense spot focus of the PFC lens and relies on some means of active thermal

management at Earth and Venus conditions. This is due to the thick germanium substrate characteristic of conventional solar cell growth on a crystalline substrate. During the Base Phase, a solution was developed to implement this on PFC-CTA: a simple mechanism, to actively adjust the spacing between lens blanket and PV blanket, to intentionally de-focus the concentrated light spot for lower (e.g., Earth, Venus) orbits. The nominally ~100 kW array (2 wing) point-design system developed for this study would require only four small stepper motors to move nearly 300 m^2 of total surface area (lens blanket + PV blanket area) relative to each other. In contrast, a concentrator design based on locally supporting lenses over each individual cell would require 13,560 actuators (the approximate number of cells and lenses in our point-design wing), or complicated mechanical synchronization, to move all of these lenses. PFC-CTA supports the flat tensioned blankets by a limited number of tapes terminating at each ends on the panels. The adjustment mechanism would need to be actuated only a few times over the course of a typical mission, to pre-determined positions. A dynamic feedback control system is not necessary, since the light intensity vs. orbit is known, the spacecraft operators know beforehand when to adjust the focus. Our preliminary evaluation has determined that defocus settings optimized for Venus, Earth, and orbits higher than Mars, would provide robust protection against over-heating, while a nominally focused setting provides optimal off-pointing tolerance and light transmission efficiency to maximize power production at higher orbits when light intensity is most limited.

A brassboard prototype of this mechanism was built and tested during the Base Phase, to validate the expected high actuation efficiency achieved by decoupling the blanket tension loads from the actuator motion by using rollers on the trolleys which bear on hard tracks on the blanket panels. The rollers offer very little resistance to the trolleys' actuation, ensuring that the torque needed to move the trolleys is very small, and the drive shaft can likewise be small and lightweight, and a small motor can be used to actuate a large number of trolleys (blanket tapes). On the small brassboard, the torque required to actuate four trolleys, each supporting 15 lbf (67 N) of tension was approximately .25 lbf*in (.03 N*m). This mechanism is expected to be robust in launch vibration, as the components are lightweight and do not support any external loads when the blanket is stowed.

The ability to de-focus the lenses is a truly enabling feature for PFC-CTA, as it is a simple yet effective throttle for the solar cell temperature to avoid over-heating, and also for enabling optimum operation - maximum power out when most needed – or *all throughout* the extremely wide range of solar intensities, from Venus to Saturn (and beyond), with essentially *standard, state-of-the-practice (TRL 9) PV cells*.

During the Option 1 phase Orbital ATK and partner SolAero developed Inverted Metamorphic (IMM) cells which have been shown (by analysis) to be much more effective at spreading heat across the PV cell and into the radiator, which would eliminate the need for active defocusing, even at lower orbits. This is the tradeoff that must be made, adopting more effective (yet lower TRL and likely heavier) PV configurations in exchange for the simplicity of eliminating the defocus mechanism. For the Base Phase, the PFC team consciously decided to baseline the design around flight-proven, "standard" PV cell configurations – materials and dimensions because we had intended from the outset that PFC-CTA be essentially agnostic to PV configurations, to ensure that the PV supplier base be unconstrained and to eliminate the dependence of PFC-CTA's viability on advancing the TRL of PV cells having integral heat spreaders. Still, this is a trade worth considering, and certainly merits a preliminary investigation such as re-running thermal models which include heat spreading features such have been demonstrated on terrestrial solar arrays and which show promise for use in space flight.

Risk I.D. 4: Given that stowed PFC lens blanket has not been tested, there is the possibility that a PFC blanket is damaged by stowage and/or dynamic (vibration) environments

Surviving the harsh dynamic launch environment is a well-known challenge for all spacecraft components, especially large, lightweight structures with high expansion ratios. The PFC blanket, in particular, comprises a large number of thin, fragile (glass), and complicated elements interconnected by slender, lightweight composite frames, and is stowed to an extremely compact volume. These factors all indicate the high value of performing a risk mitigation test on a high-fidelity, yet non-flight test article, to mitigate the risk this challenge would present to a flight program. The goal of the vibration test is to determine the survivability of a section of panel when stowed for launch. The survivability is determined by the successful deployment of the PFC blanket e.g., no snagging or sticking, and visual inspection of the hardware for damage e.g., broken lattice, untied tows, scratched or fractured lenses, and an IV continuity check of the PV cells. Fortunately, PFC-CTA incorporates a number of features that have been proven to survive launch dynamics, and additionally features, notably the composite grid frames discussed above, that support the in- and out-of-plane stowed blanket loads, and eliminate stowed pressure contact that prevent the delicate lenses from damage, lending confidence to the likelihood that the stowed blanket will survive launch and successfully deploy with zero degradation. PFC EESP Option 1 tested a representative blanket stack subjected to a simulated launch vibration environment to contribute to achieving TRL 5 for this Technology Element.

The representative blanket stack consists of four lens and PV grid panels. When stowed the lens grid panels lay on top of the front facing side of the PV grid. The grid panels are then folded into the pattern $[PV/Lens/Lens/PV]_s$ in which the outer PV grids are in contact with the end blanket panel, the backside of the inner PV grids are in contact with one another, and both of the internal lens grids are in contact with one another. SolAero provided one entire grid panel populated with live PV cells. The grid was placed second from the top in the stacking sequence. Aluminum simulators, sized to match the thickness and mass of the PV cells, were used to populate the remaining three PV grids. In the case of the lens grid panels two of the four panels consist of titanium mesh, stainless mesh, glass mesh, and 2 mil glass superstrate. The top two lens grid panels are populated with lenses, one of which is front of the SolAero PV grid. Do to the limited number of lenses an optimum assembly sequence was used that would ideally test the lens to lens and lens to PV contact when stored during the vibration test. Compatibility of similar lenses types in the stowed stack-up was tested by mirror-imaging the assembly sequence on the adjacent lens grid. The remaining two lens grids were populated with clear film simulating the mass and thickness of a real lens.

The stored blanket panel tooling used for the vibration test is an idealized representation of a full wing's stowed blanket. FEA analysis of the structure ensured the idealized stored vibration tooling was sufficiently stiff for testing the survivability of the stowed PFC blanket lens, Figure 8. The vibration test is used to also validate several important storage design features, the blanket constraints that prevent in-plane movement and the geometry of the blanket panel. Eight brackets are placed on both sides of the long axis edge of the blanket panel. The width of the aluminum blanket panel is equal to that of the composite grid frames which allows the brackets to lay against the edge of the grid frames preventing any short axis displacement. The tabs on the long axis edge of the lens grid frames stick out beyond the blanket panel. The eight brackets are place next to the tabs to constrain the composite grid frames from moving in the long axis direction. Furthermore, the brackets help in the deployment and storage of the grid frames by constraining the panels from slipping which could result in snags or deployment failure.

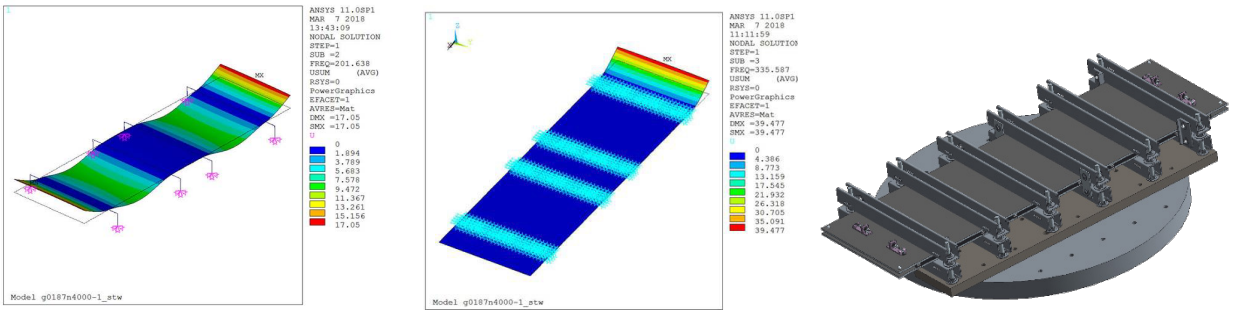

Figure 8. FEA of Blanket Test Fixture (left) and Final Design (right)

The prototype blanket panel was subjected to a representative launch random vibration spectrum at -12/-6/-3/0 dB for 20 secs in the out of plane and then short axis in-plane direction (Figure 9). This spectrum was determined by NASA during the SEP-SAS MegaFlex program, and was intended to envelope likely launcher conditions. The vibration input was controlled in two locations off of the blanket panel depicted in Figure 10 below by C1 and C2. This was to insure the idealized vibration tooling was subjecting the blanket panels to the flight vibration spectrum. Four three degree accelerometers were placed on the top blanket panel, R1 and R4 on the cantilever edge section, and R2 and R3 near the inner U channel section. A sign input of 0.5 G-peak was conducted pre and post in-plane and out of plane tests to insure the vibe tooling had not been compromised e.g., due to loosening of fasteners. Inspection of the blanket grid panel between out of plane and in-plane testing showed no signs of failure of the lens or composite grids. Visual inspection of the PV appeared to be intact as well. Full deployment was conducted at Orbital ATK on completion of the in-plane short axis test. The blanket panel deployed smoothly without sticking or snagging. Furthermore, all composite grid panels' bonds remained intact and tied to the blanket tapes. All lenses showed no signs of wear, puncture, fracture or de-bonding. The PV cells passed visual inspection and individual cell IV tests, however, the IV continuity test across the entire grid found a failure in the flex circuit soldered joint. Prior to storage and vibration testing it was observed that one of the flex circuit soldered joints had failed which could have happened during shipping and handling, assembly, or deployment prior to vibe test. The joints are found to fail easy. It is believed that failure of the joint is not directly caused by the vibration test and may have resulted during deployment and storage of the blanket panels. A means of reinforcing of the joints is essential for successful deployment and will be investigated in the next phase of the project.

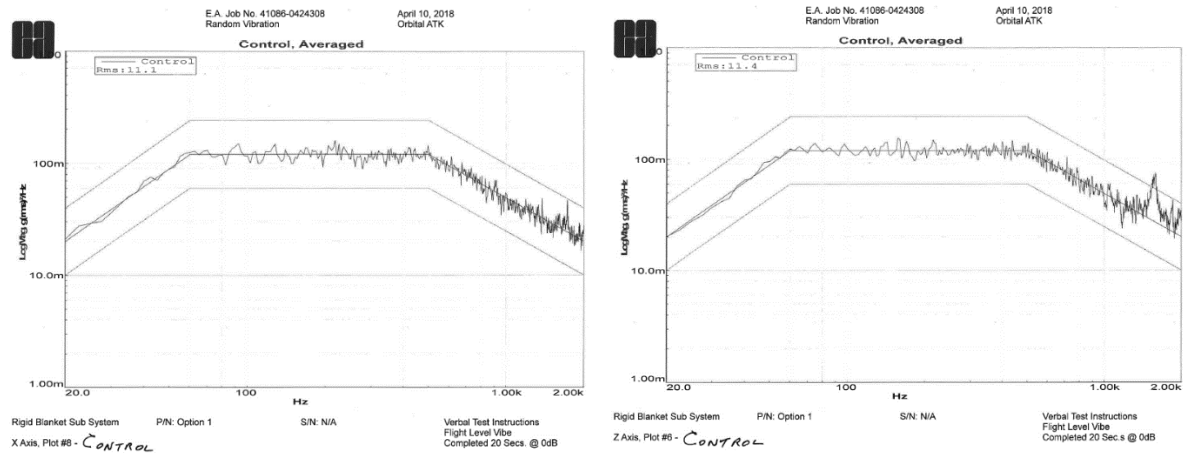

Figure 9. X- and Z-axis Random Vibration

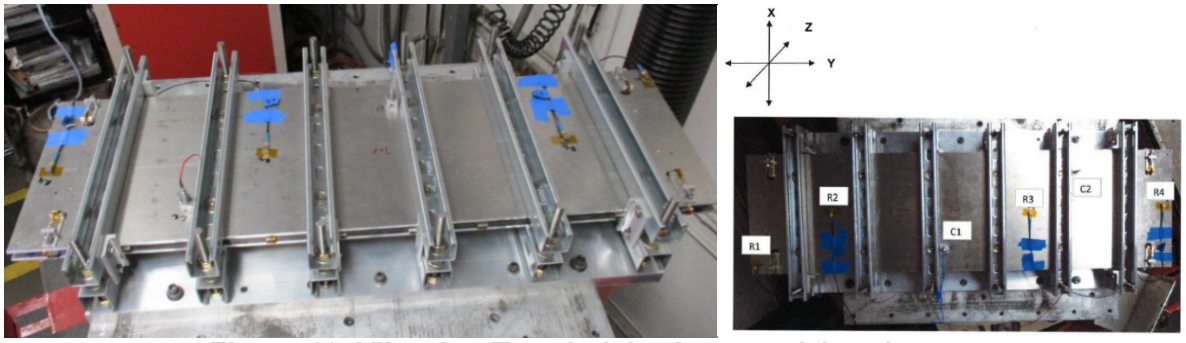

Figure 10. Vibration Test Article, Axes, and Accelerometers

The representative four PFC blanket panel stowed using idealized tooling passed flight spectrum vibration testing at a max of 0dB (full input level).

After vibration testing, the PFC blanket was deployed. Using a simple hoist arrangement to simulate the motion of blanket panels produced by the deployment of a CTA wing, the top blanket panel was raised, and the blanket allowed to unfurl. This test served to identify any possible hang-ups or sticking between blanket panels (e.g., lens-lens, lens-PV, PV-PV), damage to the flex circuit, blanket tapes, or composite grid frames. The blanket panels were deployed and inspected, with no evident damage to the composite grid frames, blanket tapes, PV, and lenses, including the four glass superstrate lenses. The test demonstrated that the PFC blanket is compatible with the launch environment, a significant achievement for this novel, high-performance design. The test blanket deployment is shown in Figure 11.

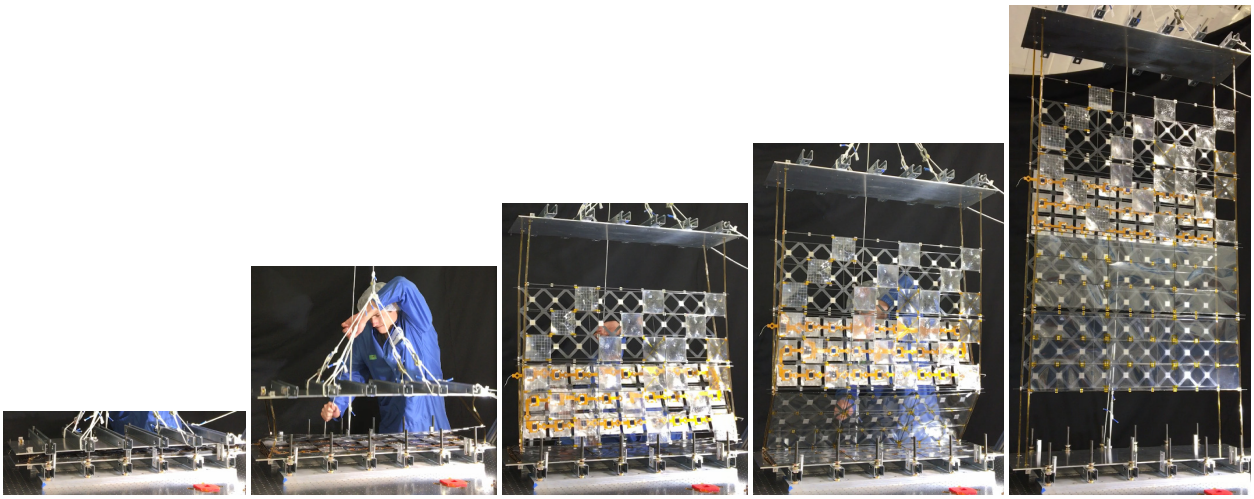

Figure 11. Blanket Deployment after Vibration Testing

Risk I.D. 5: Given that they have not yet been tested, there is the possibility that PFC lenses and/or PV cells don't survive deployed environments

Outer space poses a notoriously challenging environment, potentially damaging or distorting materials and assemblies. The key environments related to PFC are radiation (UV and high energy), electric propulsion ion plume, and wide thermal extremes (hot and cold).

Due to the extensive use of flight heritage materials and processes throughout the **CTA platform**, these deployed environments have been validated with all the same, or very similar, materials and configurations. This lends confidence to applying a relatively low risk of successfully qualifying the first PFC-CTA system for space flight.

The **lens blanket assembly** is also constructed of materials that have been extensively flown in space. However, it is clear that the lens materials are implemented much differently than typically; for example, silicone optics have been flown on multiple occasions, but none to-date in the precisely same configuration as the PFC baseline: square, flat silicone lenses, optionally with mesh reinforcement, mounted within composite grid frames. Therefore, we have looked closely at how this system performs in the relevant space environments, principally, the thermal extremes (stress and strain) and radiation (mechanical and optical degradation). A selection of lens systems were selected and prototyped (Figure 12) base on the trade study presented in Table 5.

Thermal: A detailed thermal model of the deployed lens and PV blanket was developed during the Base Phase, which included all pertinent geometry and material properties, and was used to predict temperatures of all the components at a wide range of operating conditions, primarily evaluating cell average and peak temperatures at Venus and Jupiter solar intensities. These thermal analyses were updated during the Option 1 phase to reflect a PV design based on 4J IMM cells mounted to a heat spreading substrate, as this configuration promises to effectively manage the high intensity of Venus orbit, while also offering improved electrical conversion efficiency and reduced susceptibility to radiation damage caused by operation near Jupiter.

The predicted lens temperatures were also used as the basis for lens and composite grid testing, to validate the survivability of these designs. Ti mesh lens samples were built by MOLLC and assembled into a lens grid array (Figure 13) and tested to +30C/-180C for ten cycles. Thermal cycling of the PV modules on the grid frame substrate was not performed in Option 1, but would be performed during flight qualification. This is considered a low risk test, as PV panels have been previously qualified in similar configurations.

Given the challenge of managing the large CTE mismatch between lens and grid frame, a lens mounting configuration to eliminate thermal stresses in the lens entirely has been considered, by allowing the lens to freely expand and contract independently of the grid frame. A number of concepts to accomplish this condition were considered, including a compliant connection between the lens perimeter and grid (“trampoline mount”), or by trapping the lens between two layers of fiber strands (“sandwich mount”). The “trampoline mount” poses a number of challenges, not least of which being how to achieve a compliant yet robust connection around the full perimeter, which does not result in significant loss in light collection area (fill factor). The latter method (“sandwich mount”) is appealing for several reasons, including that it ensures that the lens stays centered over the opposing cell (by attaching the lens to the strands at its center) and that the fiber strands could be made to block a minimum of light, and the lens could be almost as large as the grid frame apertures for minimal loss of collected light. Conversely, the “sandwich mount” is problematic due to concerns that the lens may bulge or crinkle as it expands at hot temperatures due to any adhesion between the lens and the support strands, unless the lens possesses adequate in-plane strength to overcome these loads. A modified “trampoline mount” was ultimately selected wherein the lens is slightly oversized vs. the four corner attachment points, and is slack at elevated temperatures, and this slack is used at cold operation to allow the lens to freely contract, minimizing load transfer between lens and grid frame, both of which could cause high stresses and/or distortions in the lens grid.

Related to thermal survivability is potential susceptibility of concentration optics to degradation by condensation of volatile solids outgassing from other spacecraft components, especially those on the solar array. This problem has plagued reflective concentrator arrays flown to date[5], while refractive concentrators, notably SCARLET and PASP+, have not experienced this type of degradation, and is therefore not expected to pose a threat to PFC-CTA.

Table 5. Lens Reinforcement Trade Study

Criteria	50-100 µm Glass Superstrate	Score	Ti mesh, suspension mount	Score
Manufacturability	Prototype lenses successfully produced with 50 and 100 um CMG superstrates.	6	Mesh-reinforced lens manufacturing appears most scalable and highest yields.	8
Lens assy (initial) inputs cost	Glass cost is insignificant (~$30/lens)	7	Mesh is inexpensive.	5
Ground Handling	Glass may crack during handling but cracks do not degrade optics	6	Mesh reinforced lenses are robust to handling.	8
Assembly/ Tooling	Glass is delicate but does not require special tooling or assembly features	8	Simple 4-point attachment facilitates assembly and replacement (if damaged)	8
Stowed launch survival	No damage on all 4, 50um lenses in Option 1 blanket vibration test. Similar glass superstrate lenses proven by SCARLET.	7	Mesh reinforced lenses are extremely robust, and no damage on any of the 9 mesh lenses tested with mini-blanket.	8
On-orbit flatness/stability	SCARLET heritage is prooGood CTE match between glass & frames ensures minimal distortion.	8	Optical efficiency at low temp questionable and difficult to test.	6
Minimal light blockage	Trivial blockage from glass.	9	~4% blockage due to mesh (not including possible cold distortion effects)	7
Robust support of weak silicone prisms	Yes, assuming glass does not crack during launch or deployment	8	Promising results from testing of small coupon but additional combined effects testing is required.	6
On-orbit UV protection of silicone prisms	Glass provides proven UV protection to silicone.	10	UVR coating shows promise but limited heritage and likely intolerant to SEP plume.	6
Plume erosion tolerance	Glass proven to survive plume without damage.	9	UVR coating will be removed by any direct plume impingement.	4
System Mass	4 mil glass on 4 mil silicone = .8 kg/m2 blanket	6	2 mil Ti mesh on 4 mil silicone = .55 kg/m2 blanket	10
Total Score		84		76

Figure 12. Lens Prototypes Produced

Figure 13. Thermal Testing Lens Grid with Ti and Stainless Mesh Lenses

Radiation: The refractive concentrators used for PFC-CTA have been under development by NASA and MOLLC and other organizations for more than three decades (see Figure 14). The lenses have proven to be robust in the simulated space environment (ground testing) by many organizations, including NASA Glenn, NASA Marshall, Orbital ATK, Boeing, Auburn University, and others. Ground testing has included monatomic oxygen exposure, space solar ultraviolet (UV) exposure, micrometeoroid exposure, electron exposure, proton exposure, thermal cycling, etc. In addition, multiple flight tests have shown the lenses to be robust in various orbits, including the high-radiation PASP+ mission (USAF and NASA) in 1994-1995, the deep space DS1 mission (NASA/JPL) in 1998-2001[6], low earth orbit (LEO) testing on the International Space Station (multiple MISSE experiments with durations up to 4 years), and the high-radiation TacSat 4 mission[7,8] (NRL/MDA/NASA) in 2011-2012. All of the lenses held up well in all of these missions and flight tests, except for a mechanical failure issue on TacSat 4, which has since been diagnosed and solved. The silicone lenses are robust when equipped with a UV-rejection coating that reflects away vacuum ultraviolet (VUV) wavelengths below 300 nm, or, alternatively, with a UV-absorbing ceria-doped glass superstrate. Many papers have been published showing these results[9]. More recently, additional testing has been performed for proton and electron exposure for missions including 15 years on geostationary orbit (GEO) and 1 year on the TacSat 4 orbit. The basic lens material (DC 93-500) was originally selected based on its half-century successful flight heritage as the cover glass adhesive on one-sun arrays in space and unique properties[10,11,12]. The latest lenses (line-focus and point-focus) developed by MOLLC for NASA in 2014-2017[13,14] include strengthening elements (either embedded mesh or transparent superstrates) and are the lightest, most robust lenses yet offered. Based on this extensive ground test and space flight heritage, Orbital ATK is confident that robust point-focus lenses can be produced to populate the PFC-CTA solar array.

Dense Plasma from Electric Propulsion Ion Plume: While certainly a “relevant environment” for any SEP solar array, this subject is not considered a key risk to PFC development. Orbital ATK[15] and others[16,17],have investigated this subject in detail, and developed solutions to mitigate these effects which will be incorporated on PFC-CTA, including complete cell and interconnect encapsulation.

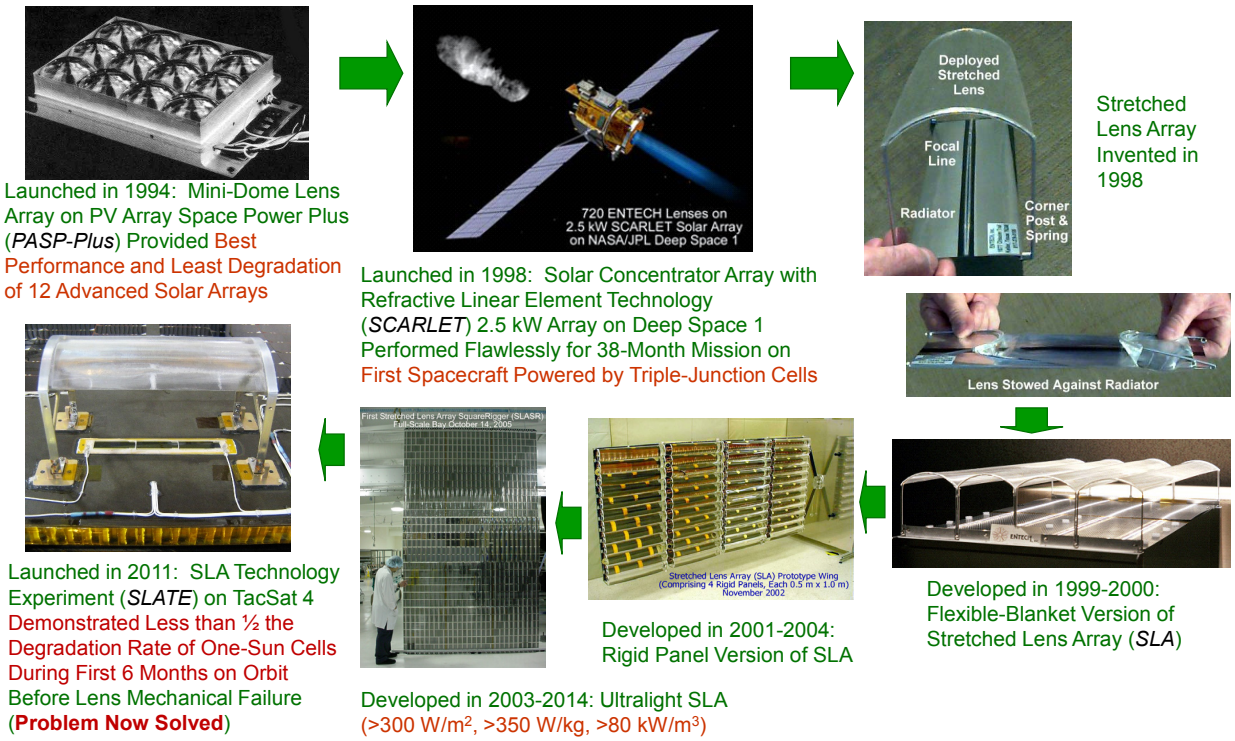

Figure 14. PFC Team's Concentrator Solar Experience Examples

Thermal Analysis

As mentioned above, thermal analysis was a key activity of the EESP Option 1 Phase. Temperature predictions for all the relevant components were used to guide the design (materials, finishes), and determine predicted performance (alignment, power production). A detailed Thermal Desktop model of the PFC-CTA blanket was developed, with model inputs and parameters corresponding to current best estimates of dimensions, materials, and properties for all relevant components. This model was run through a variety of solar intensities (orbits) and lens defocus positions. Key component temperatures were utilized by sub-system math models to determine the resultant thermal distortions that could affect system pointing. Detailed maps of temperatures over the surface of the PV cell were provided to SolAero for them to perform a grid spacing optimization (at one operating point) and power analysis of their state of the art triple junction cell at the various orbits.

Table 6 summarizes the cases evaluated and estimated power production for the 3.1-m "point design" PFC-CTA wing. Figure 15 shows the illumination on a 1/4th cell area for three selected cases.

As discussed above, one key finding of the thermal analysis was that there must be some form of active thermal management to allow a PFC 25X GCR array to fly at sub-1 AU orbit, e.g., for a Venus flyby mission assuming standard PV cells are to be used. PFC-CTA is uniquely capable of achieving this with a minimum of added complexity by defocusing the entire array of lenses with a small number of actuators and simple mechanism. The effect of defocusing the lenses is made clear by the plots of Figure 15 and Figure 16, and the point focus lens shown in Figure 17.

Table 6. Thermal Modeling Cases & Summary Results (PV temps for 3J cells)

Location	AU	"suns"	% of NFL	% light hitting cell	Spot size on cell (Øcm)	Predicted Temps (C)					Eff (%) Rel. to 1367 W/m^2	Point-Design Wing Power (kW)
						Lens & Grid	Lens Grid Front/ Back Gradient	PV Peak	PV Grid	PV Grid Font/ Back Gradient		
Venus	0.72	1.93	72	50%	2	34.6	1.0	161.8	110.6	0.3	24.4%	37.5
Earth	1.00	1.00	72	50%	2	-23.0	0.4	82.4	56.0	0.2	28.8%	22.9
Earth*	1.00	1.00	94	100%	1.4	-22.0	0.6	180.5	57.6	0.2	22.8%	36.3
Mars	1.50	0.44	94	100%	1.4	-68.0	0.3	52.7	-4.0	0.1	30.7%	21.7
Jupiter	5.20	0.04	100	100%	0.6	-161.0	0.1	-109.0	-125.0	0.1	38.0%	2.2
Saturn	9.60	0.01	100	100%	0.6	-195.0	0.1	-160.2	-165.0	0.1	39.7%	0.7

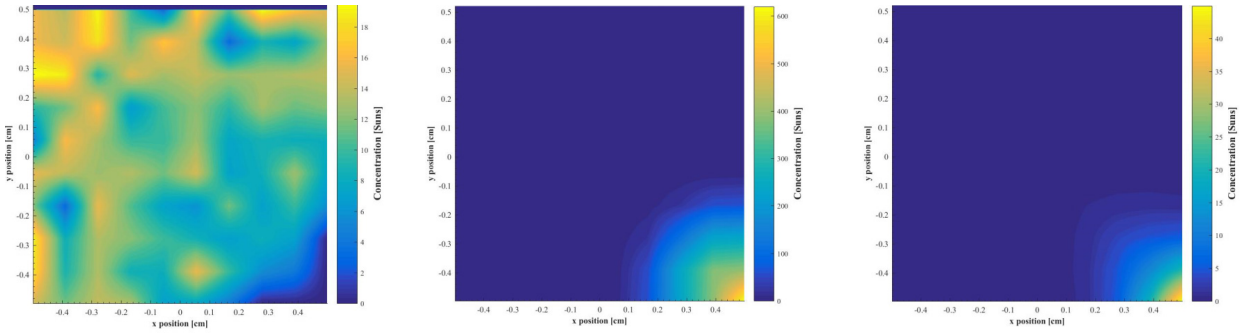

Earth, 72% FL, ¼ cell area ***Earth, 94% FL, ¼ cell area*** ***Jupiter, 100% FL, ¼ cell area***

Figure 15. Cell Illumination Examples

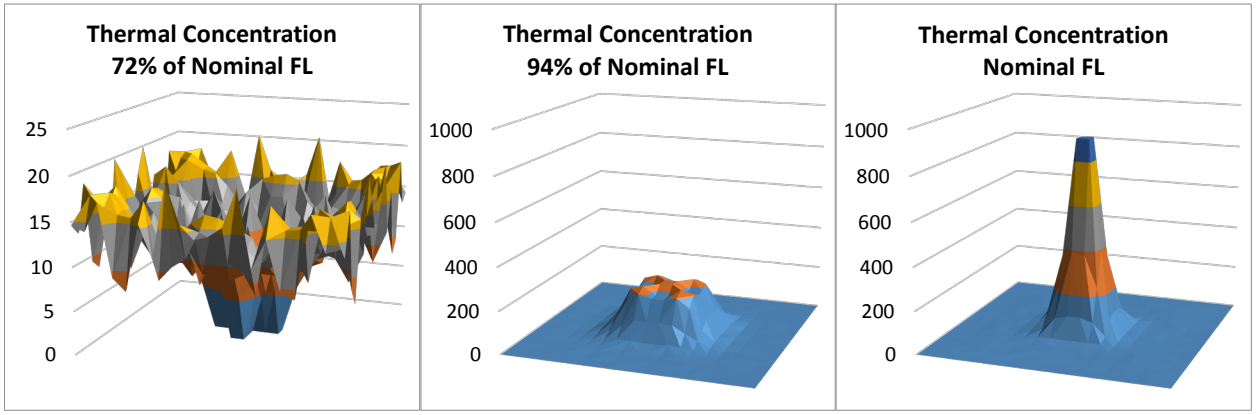

Figure 16. Light Spot on Solar Cell at Nominal and De-Focused Positions

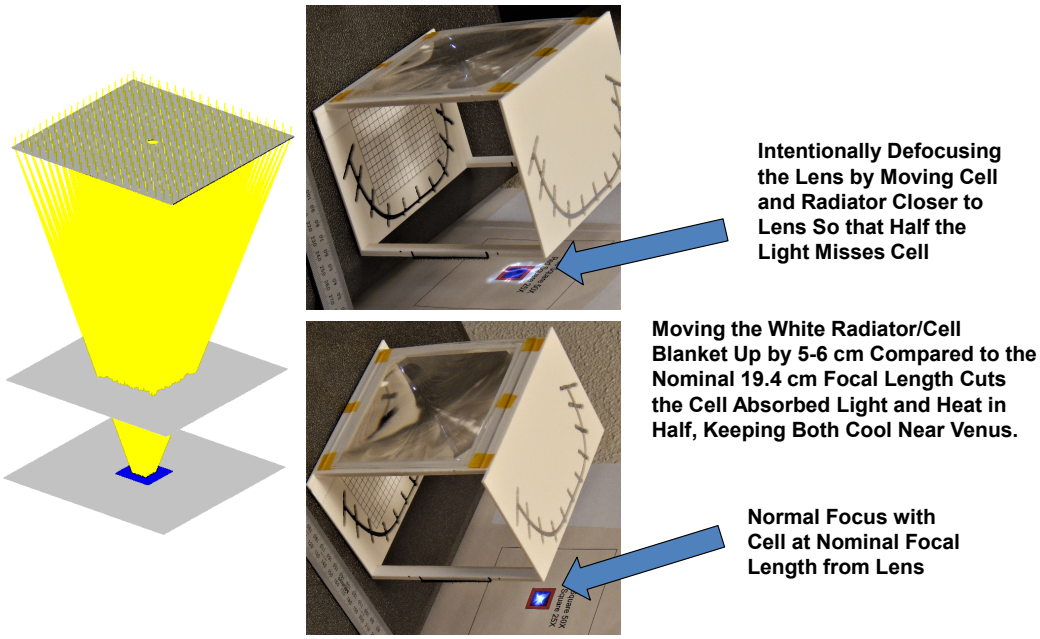

Figure 17. Effects of Lens De-focusing on Light Intensity Hitting Cell

Lens and PV Hardware Development

The base phase led to a down selection of four lens types; glass superstrate, fiberglass mesh, and two designs which utilize electroformed metal mesh made of either titanium or stainless steel. Each lens type offers unique advantages previously discussed in risk I.D. 5 above. The mechanical and optical performance of these designs were further validated during the Option 1 contract through testing that included thermal cycling of the integrated lens grid-frames and a very ambitious thermal-optical test of a functioning 25X concentrator prototype.

A representative 3x3 lens grid-frame was thermal cycled to validate the structural robustness of the composite grid-frames and pin-post lens mounting concept selected for the two metal-mesh lens types. The frame was populated with five titanium mesh lenses and four stainless steel mesh lenses. The thermal chamber was cycled between -180°C and 35°C. The frame showed significant deformation at cold, and upon further evaluation the deformation was due to stress from the high CTE stainless steel lenses. After removing the stainless steel lenses the test was repeated and the frame displayed no noticeable deformation at either temperature extreme. Ten full thermal cycles were performed with no observable damage to either the composite grid frame or the titanium lenses. This test was able to validate the selected composite grid-frame design and lens mounting concept, as well as validate stress concerns due to the high CTE of stainless steel.

A slight wrinkling of the mesh lenses was also observed at cold. This is likely due to internal stresses caused by differences in CTE between the silicone and mesh material. A qualitative optical test was performed in order to assess the impact of this wrinkling on the optical efficiency of these lenses. A small light-source was placed approximately 8 feet from the thermal chamber and shown through a glass window in the chamber door. The 3x3 lens grid was hung in the chamber so that the light shown through the window was concentrated on a focal plane, 20 cm focal distance from the lens. The illumination spot on the focal plane was photographed at hot and cold temperature extremes and qualitatively compared. These photos are shown below in Figure 18. The results reveal that the focal spot appears to tighten due to the wrinkling, however true insight on the effect of temperature on the optical efficiency of the lenses cannot be inferred from such a qualitative test. This test did however confirm that the performance of the lens is dependent on temperature to some degree.

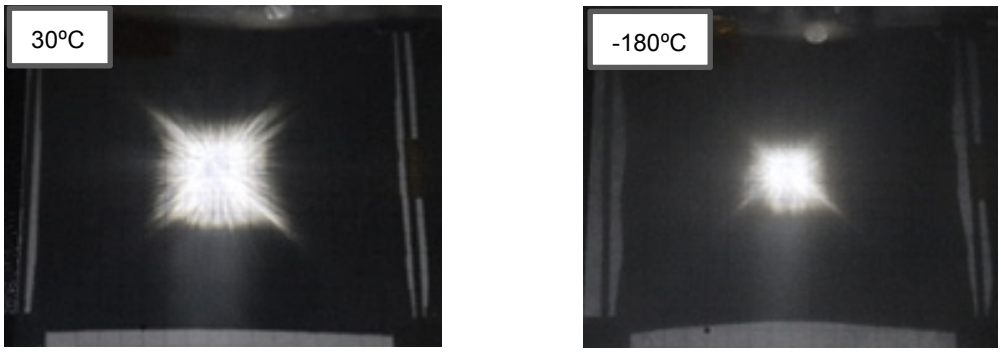

Figure 18. Photographs of Concentrated Illumination Spots at Hot and Cold

In order to quantify this effect, as well as get a better assessment of system level performance of the PFC concentrator assembly, a more comprehensive test was performed on a complete concentrator prototype system using a solar simulator and thermal vacuum chamber at SolAero. The prototype consisted of a 3D-printed concentrator frame, titanium mesh MOLCC lens, and a single complete PV assembly consisting of a CPV ZTJ CIC, flex-circuit, bypass diode, thermal radiator and composite support lattice (Figure 20). This concentrator assembly was suspended by wire inside of a Dynavac thermal vacuum chamber with a pressure less than $1e^{-6}$ Torr. Three T-type thermocouples were used to monitor temperature at the back side of the cell, front side next to the cell, and on the assembly frame. Illumination was provided using a modified XT30 Xenon arc lamp shone through a 7" borosilicate window to simulate AM0 conditions. This setup is shown below in Figure 19.

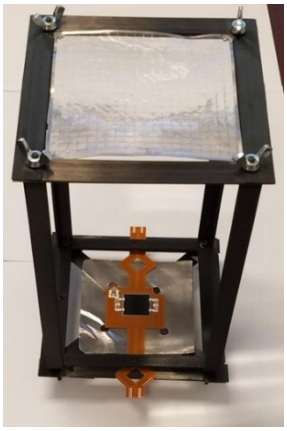

Figure 20. Concentrator Prototype

Figure 19. TVAC Optical Test Setup with Dynavac Chamber and XT-30 Solar Simulator

The prototype assembly was initially illuminated at ambient conditions with the lens removed for a baseline measurement for determining concentration factor. The lens was placed back onto the system and ambient and vacuum concentration tests began. The results expressed a concentration factor of 13.6X. This was substantially below the expected concentration factor of 20-25X. This lower than desired result was not due to poor concentrator prototype performance, but rather to testing limitations. The XT30 solar simulator was placed too close to the concentration assembly and the resultant illumination was highly non-collimated. Ray-tracing simulations performed corroborate the measured results and the source of this lower than anticipated performance. Figure 21, below shows the measured result falling in line with the predicted performance curve. Significant improvements to this test can be made by increasing the working distance of the light source to increase collimation and adjusting the lens/cell focal length to account for the remaining non-collimation.

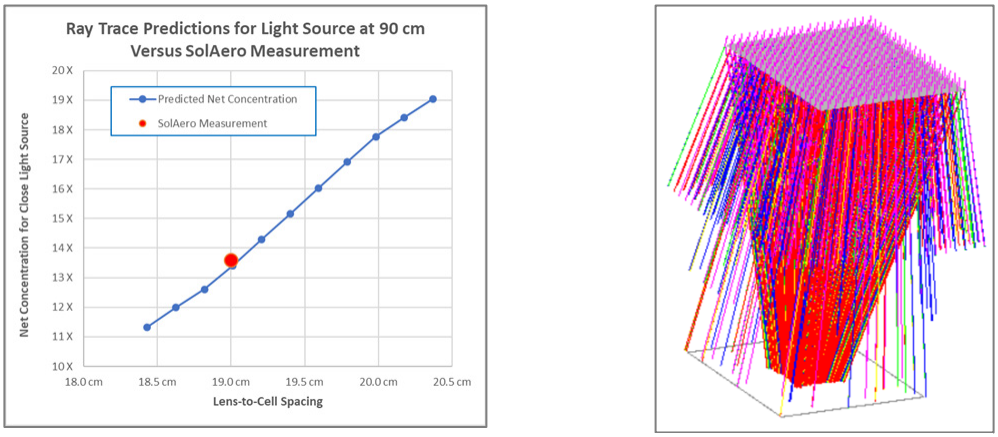

Figure 21. Ray Tracing Model and Prediction for Concentrator Performance under Close-Proximity Source

Although the collimation of the solar simulator was not ideal for determining concentration performance, the comprehensiveness of this test enabled invaluable insight into other system performance metrics of the prototype design. IV curves for the PV cell under concentration are shown below in Figure 22 at varying temperatures measured by the frame. At first inspection, there appeared to be a trend of increased ISC with temperature. However, upon applying a temperature correction to the current production of the cells, the trend reversed and there is a slight decrease in current production. This correlates with what was observed in the qualitative thermal optical test, and suggests that as the lens wrinkles under internal thermal stresses, the spot size, or perhaps the focal length, decreases.

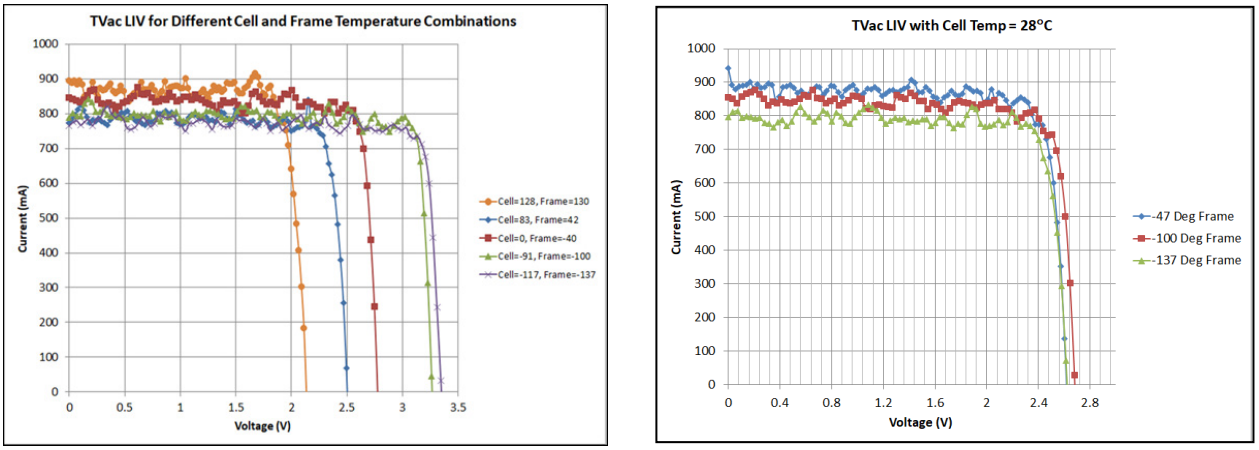

Figure 22. IV Curves Taken During TVAC Concentration Testing

This test also enabled us to measure the performance of the thermal radiator attached to the CPV assembly by performing a rudimentary thermal balance test. The XT30 solar simulator is a light source that is capable of continuous illumination. The TVAC chamber temperature was lowered until the thermocouple on the frame read between -125 and -130°C. Then the prototype was illuminated until the cell reached steady state temperature. Figure 23 below shows that the front of the cell reached approximately 160°C.

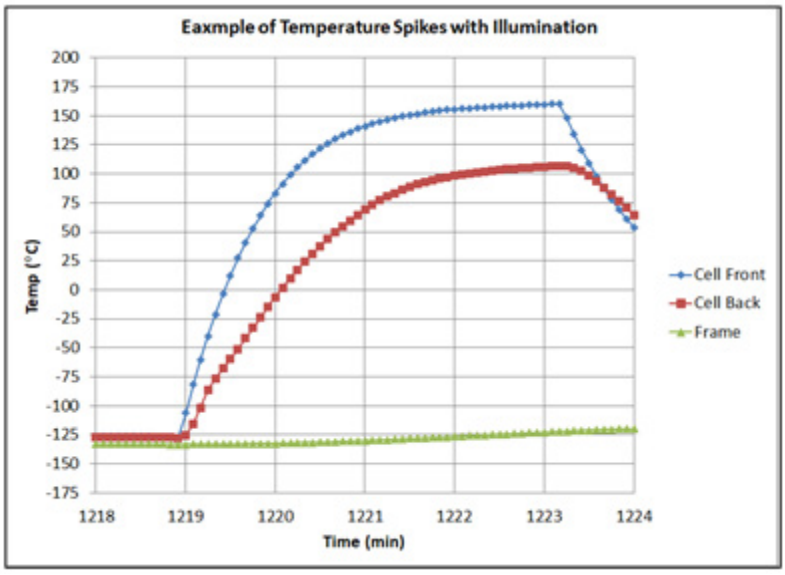

Figure 23. Prototype TC Measurements Under Continuous Illumination

Analysis of this bare thermal radiator under 1AU concentration and at the VOC point predicts a cell temperature of 164°C, correlating very closely with the measured result. This analysis along with extrapolations for the performance of radiators coated to improve emissivity are summarized in Table 7, below. The agreement between predictions in measurement gives us confidence in our design and manufacturing as well as our ability to predict behavior of this system as new design options are considered.

Table 7. Radiator Thermal Analysis

Sigma	A-radiator	Irradiance	Tau-lens	Alpha-cell	Cell Eff @25C	Cell Eff @T-rad
5.67E-08 W/sq.m.-K^4	100.0 sq.cm.	0.1366 W.sq.cm.	90%	95%	0%	0%
T-space	Emit-rad	Emit-lens	Total Emit Factor	Waste Heat Rate	Waste Heat Flux	Sigma x A x Emit Factor
4 K	33%	90%	57%	11.6793 W	1167.93 W/sq.m.	3.20443E-10 W/K^4

T-rad-avg	T-rad-avg
437 K	164 C

Condition	Radiator Emittance	Average Radiator Temperature
1 AU VOC	70%	99 C
1 AU Peak Power	70%	70 C
1 AU VOC	33%	164 C
1 AU Peak Power	33%	136 C

Additional extrapolations were made to predict performance at the 5AU, -125°C environment designated by the EESP Success Criteria. This analysis predicts an average radiator temperature of -132°C under illumination, which is slightly below the optimal temperature of -120°C. MOLCC is currently developing an enhanced radiator technology through a NASA STTR with the University of Connecticut. This technology combines thermally conductive material of varying thickness deposited directly onto aluminum foil that allows the radiator surface to curl at cold temperatures, reducing its view factor to deep space and thus preventing the cell from dropping below a desired temperature. This technology could help to maintain optimal temperature for the PFC-CTA array, as well as improve CIC/radiator manufacturability, discussed in more detail below. An image of the current prototype at cold temperature is shown below in Figure 24.

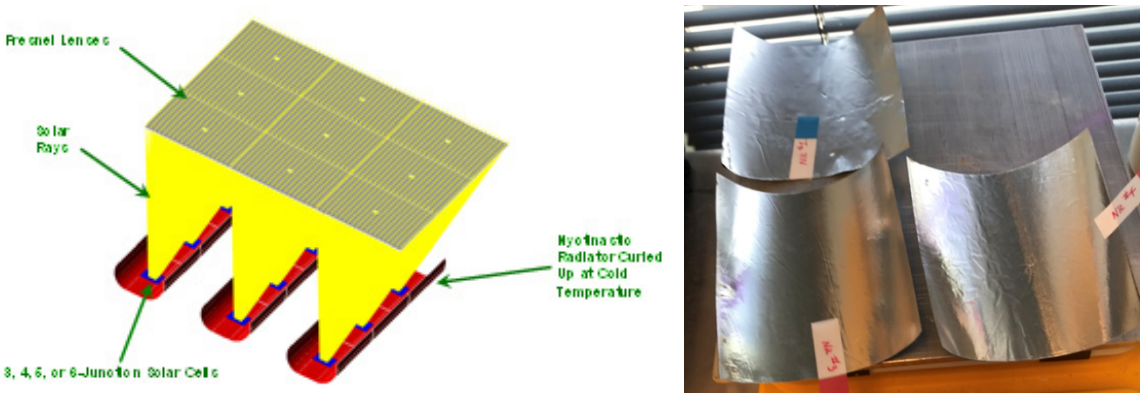

Figure 24. Simulation of Nyctinastic Radiator Behavior and Prototype Radiator

This Option 1 work was also able to benefit from lens optical efficiency testing performed by MOLCC on their CCRPP program, contract number 80NSSC17C0073. MOLCC recently reported an optical efficiency of 90% for glass superstrate lenses and 84% for the titanium mesh lens design during outdoor optical testing. MOLCC was also able to further evaluate the system level performance of this lens technology during their CCRPP program through LAPSS testing a prototype 25X concentrator system at SolAero. While there were issues with the performance of the 3J concentration cells developed by SolAero, the lens and cell performed well as a concentration system and the causes of the sub-optimal cell performance were identified. The identification of these developmental issues allowed MOLCC and SolAero to extrapolate the expected performance of this 25X concentration system for future applications. The results of this extrapolation are summarized in Table 8 below.

Table 8. Extrapolated EOL Performance

Item	Recent LAPSS Results*	Correct Grid Width*	Reduce Emitter Sheet Resistance*	Add Prismatic Cell Cover*	Improved Lens*	Future 4J Cell*	Extrapolate to 5 AU***	EOL Performance at 5 AU
Cell Efficiency	25.8%	26.6%	27.4%	29.8%	29.8%	35.0%	45.2%	40.6%
Lens Efficiency (CMG/Silicone Lens)	85.0%	85.0%	85.0%	85.0%	90.0%	90.0%	90.0%	88.2%
Concentrator Module Efficiency (CMG/Silicone Lens)	21.9%	22.6%	23.3%	25.4%	26.9% **	31.5%	40.6%	35.8%
Concentrator Module Efficiency (Mesh/Silicone Lens)							38.4%	33.8%
Footnotes:								
*at 25C, 1AU AM0, 1,353 W/sq.m.								
** > 27% Demonstrated in 2014 for Earlier 25X Concentrator								
***at -120C, 5AU AM0, 54 W/sq.m.								

With the application of correction factors for oversized grid-lines, unexpectedly high emitter sheet resistance, prismatic cell covers, and MOLCC's improved lenses, as well as estimates for the efficiency of the concentration optimized IMM4 cell technology developed over the course of this Option 1 contract, the 25X concentrator system promises an impressive BOL efficiency of 40.6% to 38.4% at 5AU, -125°C, and 54W/m^2. This greatly exceeds the success criteria goal of 33-25% BOL cell efficiency.

The EOL performance estimates highlight one of the hallmark advantages of using concentrator arrays. Due to the small total area of active PV within this 25X concentrator system, significant thickening of the protective cover glass, and thus increased shielding, can be achieved with minimal mass penalty to the array performance metrics. The EESP "Success Criteria" specifies EOL performance to be determined after experiencing an equivalent fluence of 4 x 10^{15} 1 MeV e^-/cm^2 for the total mission radiation exposure. According to recently published IMM4 radiation testing from the JPL and SolAero EESP Base Phase Report[18], this level of fluence will result in approximately a 76% EOL efficiency for the 5AU and -125°C

environmental conditions. However, the 2012 IECEC paper, "JUNO Photovoltaic Power at Jupiter", by Dawson et al.[19] reveals that by increasing cover-glass thickness on the PFC photovoltaics to 30 mils, the equivalent radiation fluence experienced by the photovoltaics is reduced to 2 x 10^{15} 1 MeV e^-/cm. Applying this new metric to the IMM4 radiation test data predicts an impressive EOL cell efficiency of approximately 88% for one-sun illumination and 90% for 10-sun illumination. Extrapolating 10-sun -125°C IMM4 efficiency testing to 25X concentration produces a BOL cell efficiency prediction of 45% and thus an EOL prediction of ~40%. The extrapolation is shown on top of the results found in the JPL EESP Base Phase[18] below in Figure 25.

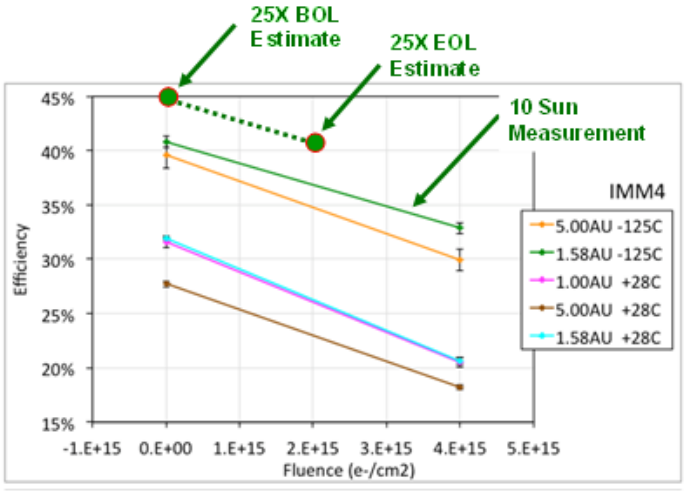

Figure 25. IMM4 Radiation Test Results and Extrapolations for PFC Concentration

Additionally MOLCC has performed radiation degradation testing on their silicon lenses with embedded metal mesh. Dawson et al. calls for an equivalent proton fluence of 1.1 x 10^{14} 50 KeV p^+/cm^2 for the Jupiter environment. MOLCC's silicone lenses have previously been tested at 10X this fluence with 30KeV protons, showing less than a 2% degradation in transmittance[12], results shown in Figure 26. Combining the small effect of this equivalent fluence on lens performance with the previously predicted EOL performance of the IMM4 cell technology, the estimated EOL efficiency of the concentrator assembly is approximately 33-35%. Just as is the case for BOL performance of this concentrator system, this EOL efficiency substantially surpasses the EESP Success Criteria goal of 25-28%.

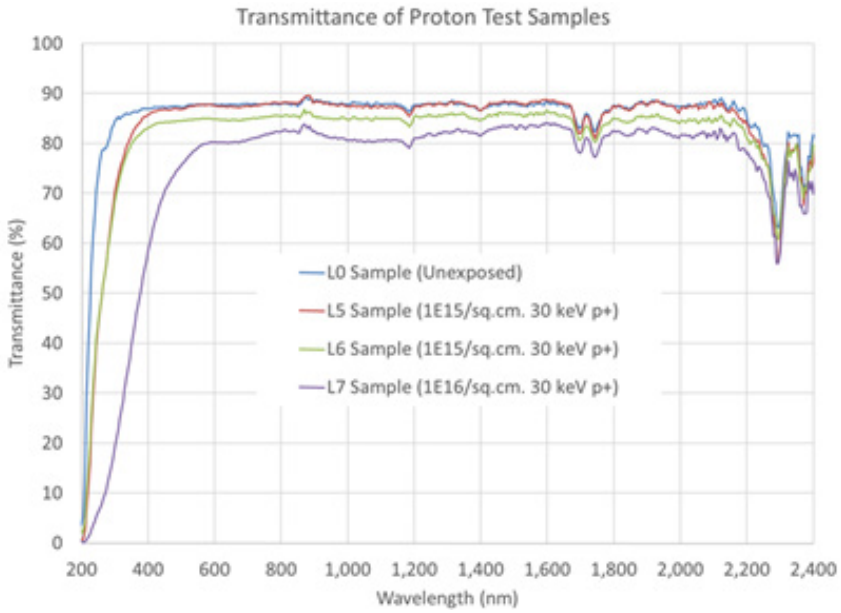

Figure 26. MOLCC Silicone Lens Radiation Testing

In order to advance the TRL of this technology from 4 to 5, Orbital ATK partnered with SolAero to develop and manufacture a fully populated and active PV module that included thermal radiators. This module consisted of 27 CIC's strung together in a 3x9 matrix integrated into a composite PV lattice grid, built by Orbital ATK. The delivered prototype is shown in Figure 27, below.

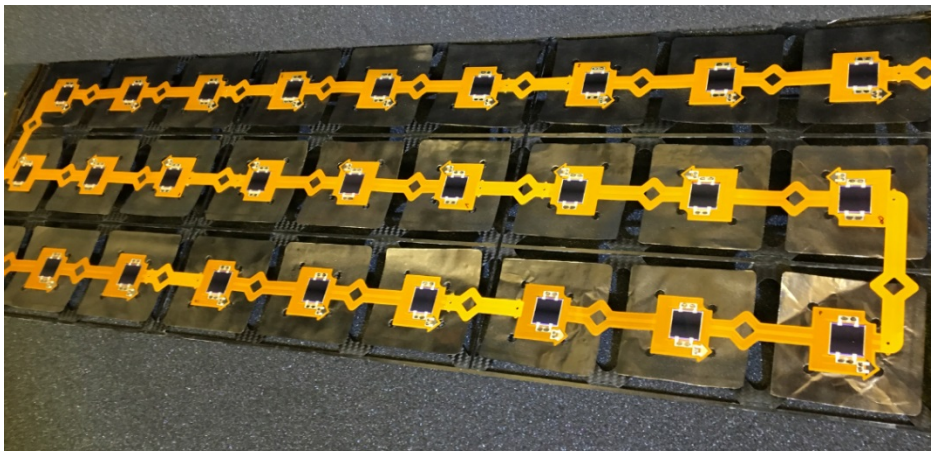

Figure 27. Composite PV Module

During this development Orbital ATK and SolAero focused on both functionality and manufacturability of the PV module. It is often assumed that concentrator arrays lend themselves to manufacturing challenges, however the increased distance between cells and the modularity of the design produced during this Option 1 in fact offer many manufacturing benefits. This PV module utilized a modular flex-circuit design that allowed for fixturing and reflow solder techniques that simplified and expedited the manufacturing process as well as provided a clear path for scaling. The large cell-to-cell spacing allowed for increased mechanical isolation and strain relief between CICs, providing clear advantages when compared to the IC stress concerns and cell-rework accessibility associated with traditional densely packed array designs.

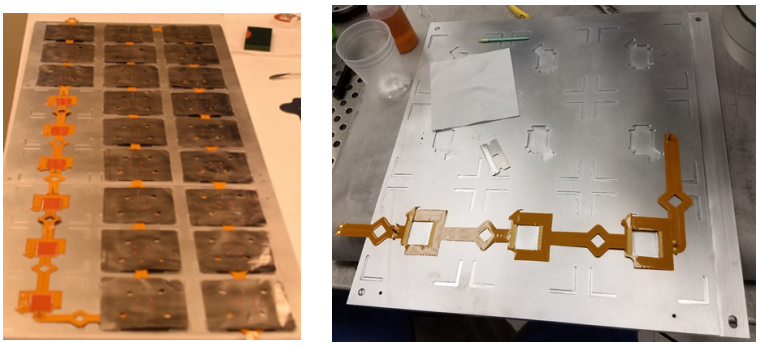

Figure 28. Flex-Circuit and String Assembly Fixtures

Additionally SolAero developed both 3J and 4J PV technology to be used in this concentration system. Based on the in-depth thermal modeling performed by SolAero, a mask set was procured for processing both ZTJ and IMM4 epitaxial material into solar cells. Both ZTJ and IMM4 materials were modified to optimize concertation performance by increasing current capacity of the tunnel diodes and reducing the top junction sheet resistance. The front grid lines were also redesigned to account for the specified concentration profile. Two lots of ZTJ cells and one lot of IMM cells were produced.

A detailed process for integrating the cells into the flex-circuit harness and then the composite lattice was developed for both ZTJ and IMM4 technologies. Graphite fixturing was made in order to attach the AlN heat-spreaders to the ZTJ cells, whereas AlN was able to be attached to the IMM4 cells during processing of the wafers. The initial lot of ZTJ cells was selected for integration into the 27 cell PV module. CICs were assembled into their 1x3 sub-circuits and then integrated into a large aluminum string assembly fixture where flex-circuit connectors were soldered to complete the string circuit (See Figure 28).

System-Level Performance Analysis

A system sizing spreadsheet has been developed and updated by Orbital ATK to incorporate all relevant solar array parameters, constraints (e.g., stiffness, strength, maximum dimensions), and goals/objectives (e.g., max W/kg or kW/m^3) to allow the user to quickly perform “one-click” system optimization and sizing of the wing. The spreadsheet provides all the relevant dimensions, including mast components (longeron and diagonal width and thickness), blanket panels (facesheet and core thickness), blanket tension, etc.

These initial parameters are then easily imported to the master system CAD model, which assigns parameters to component dimensions, which in turn updates entire solar array wing. This is a powerful tool, by nearly instantly providing a high-fidelity design baseline for mission planners (spacecraft systems engineers) to optimize and iterate potential mission architectures to different aspect ratios (for example, a dual-manifest launch configuration), orbital trajectories (optimizing power production at a particular orbit/intensity), stiffness, strength, etc.

This tool has been exercised to produce a comparison between a “one-sun” CTA system and a PFC-CTA system at 25X geometric concentration ratio (GCR), which is the current study baseline. An example of the sizing tool’s utility in optimizing for a wide range of goals is the EoL $/W metric, which conceivably may be a driving requirement, especially for a very high-powered mission. Thanks to the 50% reduction in EoL power loss vs. a lightly shielded 1-Sun blanket, coupled with significantly reduce PV (solar cell) active area ($1/25^{th}$ the PV area of a 1-sun array), the EoL $/W (PV content only) estimate for PFC-CTA is approximately $1/25^{th}$ of the one-sun CTA array cost, and other critical metrics (W/kg, kW/m^3) are also substantially improved, especially at EoL. The results of this comparison are shown in Table 9.

Scaling trends can also be explored in depth, where specific power on a kW/m^3 basis or W/kg basis generally trend slightly down as wings grow, as would be expected. Tradeoffs between stowage efficiency (kW/m^3) vs. mass efficiency (W/kg) can also be made.

Table 9. Wing-Level Performance Estimates

	Metric	PFC	CTA	Notes
	Geometric Concentration	25	1	
	Coverglass & Substrate Thk (mils)	30	4	30 mils shielding on PFC adds only 0.2 kg/m^2
	Wing Active Area (m^2)	142	132	PFC has higher effective packing factor (no cell crops)
	Wing Mass (kg)	179	196	
	Blanket Areal Mass (kg/m^2)	0.77	0.89	PFC includes PV & lens blankets
	Wing Stowed Volume (m^3)	0.80	0.55	
1 AU	BoL Cell Efficiency	29.0%	31.0%	Includes temperature effect
	Solar Intensity (W/m^2)	1345	1345	
	Cell Temp (C)	90	60	
	Lens and Harness Knockdowns	86%	98%	Including lens knockdowns listed below
	Wing Power (kW)	47.8	54.1	PFC 12% lower but BoL power likely not sizing wing
	BoL W/kg	267	276	Both extremely high performance at 1 AU, BoL
	BoL kW/m^3	60	98	PFC blanket is ~2x as thick as 1-Sun
5 AU	BoL Cell Efficiency	45.2%	37.9%	Higher BoL cell % for PFC due to higher intensity
	EoL Cell Efficiency	40.7%	29.5%	30 mil shielding-->10% loss vs. 22% for 4 mil shielding
	Lens and Harness Knockdowns	84.5%	98.0%	See table below for lens knockdowns
	EoL PV/Lens Blanket Efficiency	34.4%	28.9%	Trivial lens degradation at EoL
	Solar Intensity (W/m^2)	50	50	
	EoL Wing Power (kW)	2.4	2.0	PFC delivers 25% more power at 5 AU, EoL
	EoL (W/kg)	14	10	1.8X better W/kg at EoL for PFC
$	PV Cost ($/W)	$ 800	$ 400	Assume 2x cost per area for CPV cells
	Wing PV Cost, (k$)	**$ 1,529**	$ 21,642	Concentrator reduces cell area by 95%
	PV k$/W, EoL @ 5AU	**$ 0.6**	**$ 11.1**	**~94% EoL $/W (PV) savings with PFC!**

High optical concentration solar arrays have been studied in depth by NASA scientists and engineers, and a concise summary of current thinking is offered by Geoff Landis in a recent paper[18]: “The net calculation, incorporating intensity, LILT, and radiation effects, suggests that for a 1-year mission at Europa, concentrator systems at a concentration of ~25 could produce on the order of 50% higher end-of-life power for the same array mass. For mission further into the radiation belts (e.g., Io), or longer assumed lifetimes, the advantage increases. Whether this increase in power is worth the added complexity and pointing requirements of a concentrator system is a question for the spacecraft systems engineer.” These projections are consistent, if conservative, with the findings made by the PFC-CTA study.

A summary of the projected PFC-CTA performance vs. the requirements set forth in the EESP NASA Research Announcement (NNH15ZOA001N-15GCD-C3) is provided in Table 10. Despite their aggressive, "Game-Changing" quality, all goals are readily achieved by PFC-CTA, many by a significant (~2X) factor.

Table 10. PFC-CTA Performance vs. NRA Goals/Requirements

Array System Goal (for conclusion of Option II)	Comment (as of conclusion of Option 1 Phase)
35% BOL cell efficiency measured at 5 AU and -125°C	45.2% predicted efficiency for cell operating at -130°C at 5 AU using IMM 4J cells. (Prediction includes improvements over test data by further design refinements as described in report.)
28% EOL at the blanket (or equivalent) level, given mission conditions characterized in Table 1	34.4% EoL Blanket-level efficiency (including lens knockdowns).
8-10 W/kg measured at EOL inclusive of the array structure and deployment mechanism, given mission conditions characterized in Table 1	Refined PV efficiency, lens efficiency, system mass sizing, estimate remains at 18 W/kg (same as end of Base Phase). Compare with 10 W/kg for 1-Sun CTA wing.
Packaging density of at least 60 kW/m^3(2), calculated at power level predictions for BOL in near earth orbit (1345 W/m^2)	Matured grid design and thick shielding yields 60 kW/m^3. Thinner shielding improves BoL metric, but EoL performance likely driver. 1-Sun CTA provides 98 kW/m^3 (single blanket stacks thinner).
Demonstrate ability to integrate proposed technology into a solar array structure that can be stowed and survive launch conditions.	High-fidelity PFC blanket (PV & lens, interleaved) built and vibration tested during Option 1, with no damage, including glass-superstrate lenses. Two separate Phase-2 SBIRs developing CTA architecture (hardware fabrication in work), second of which will include wing-level vibration testing.
Technology capable of operation over the range of 100 – 300 V.	Yes, protection from arcing in plasma by cell encapsulation via overlapping coverglass and edge grouting, interconnects fully encapsulated, demonstrated on MegaFlex SEP/SAS program >600V in plasma density of 10^8 cm^{-3}. 2x higher than goal. Sparse PV cell spacing and small cell area facilitates robust structure grounding and insulation of cells.
Technology capable of operation in the presence of plasma exhaust fields equivalent to Xe plasma having an energy level (Te) of 2 eV and a number density of 1e8/cm^3	PFC design incorporates high voltage isolation features to protect against damage or losses due to high-density plasma.

Technology Readiness Assessment

PFC-CTA promises game-changing performance benefits over state-of-the-practice, un-concentrated planar solar arrays for deep space use. It achieves this significant performance benefit by aggressive optical concentration obtained by ultra-lightweight flat Fresnel optics, packaged and deployed by a highly efficient truss-supported, tensioned blanket structural system. The basic components that make up the PFC-CTA system all benefit by a maturity established by multiple successful space flights; it is the system architecture and unique configuration of these components that is novel for PFC-CTA. As a result of this strong heritage, there can be a difficulty in determining a rating of TRL at the component and subsystem level.

For example, the carbon fiber struts that comprise the telescoping truss mast are constructed using the same fiber and resin material that has successfully flown on a number of missions. The difference for CTA is that these struts are formed into different profiles (L-section vs. typical round), and assembled with different bond geometry to adjacent components. For this and similar examples, the TRL is being raised by the design, building and testing of prototype hardware, and subjecting it to increasingly high fidelity simulations of the relevant space environment(s).

As is typical with spacecraft components, flight qualification of the PFC-CTA system will need to be achieved by a combination of testing, some of it performed at the sub-system level. For example, it is not possible to do a realistic wing-level electrical performance test using a solar simulator, as there are no known large-area, collimated solar simulator facilities. Therefore, it is likely that electrical verification of a PFC-CTA wing will consist of module-level testing, which would be more practical. Once integrated into the complete wing, circuit-level electrical checks can verify continuity and cell health, and would be repeated throughout environmental testing. Unique to PFC-CTA is wing-level verification of lens-to-cell alignment. This can be performed simply by using a distant light source which is scanned over the area of the deployed wing, and a qualitative (visual) assessment of light spot alignment over each cell can be made. This is actually preferable to attempting to verify alignment using a hypothetical large-area solar simulator, as this test would not demonstrate an initial alignment bias between focus spot and cell, and to direct adjustments if indicated.

Table 11 presents the maturity of the key PFC system components versus critical relevant environments highlighting the challenges overcome in Phase 1.

Table 11. Relevant Environments and Maturity of Key PFC Elements

Item(s)	Stowed Dynamics	Deployed Dynamics	Deployed Environments
Mast, blanket panels, mecha-nisms	High-fidelity EDU developed under two, Phase-2 SBIRs. Vibration testing is planned for 4Q 2017.	Mast is preloaded, determinate structure. Full-scale EDU's will provide ground test validation of high-fidelity FEA.	Pointing accuracy is key performance attribute (besides survival). Continuous, unidirectional composite elements, un-strained when stowed and deployed, in conjunction with determinate, preloaded latches, promise extremely predictable system-level behavior.
Lens Panels	Blanket design with composite grid frames is inherently robust. Vibration testing of stowed blanket coupon is planned for Option 1.	Composite grid frames have been sized to guarantee that local panel modes are much higher than blanket system. Thermal analysis indicates that crosswise bowing is insignificant.	**Thermal:** Thermal cycling and analysis of brassboard coupons indicated need for different lens support method. Many options available to investigate. **Radiation:** Results from coupon tests with similar to EESP target doses produce acceptable degradation. **Plume:** Wing geometry will minimize impingement.
PV Panels	(similar to lens panels)	(similar to lens panels)	**Thermal:** Thermal extremes predicted for PFC are encompassed by flight heritage conditions. **Radiation:** Results from coupon tests with similar to EESP target doses produce acceptable degradation. **Plume:** Wing geometry will minimize impingement.

The NASA Game Changing Development Extreme Environment Solar Power (EESP) Option 1 Phase study has enabled Orbital ATK to generate and refine component designs, perform component level and system performance analyses, and test prototype hardware of the key elements of PFC-CTA. A detailed assessment of the TRL level at the end of the Phase 1 placed the majority of the critical components at TRL 5. However, the overall system was assigned TRL 4 due to the lowest component technology readiness level. A TRL of 5 would be easily achieved with developments planned under complimentary efforts together with the activities proposed for Option 2.

Activities Related to PFC-CTA Development

While the subject EESP study focused on the challenges unique to implementing optical concentration into a CTA wing, the CTA wing itself has been actively developed primarily by a pair of Phase 2 SBIR programs, as well as others, as shown in Table 12. These SBIR programs have produced two generations of increasingly high-fidelity prototypes, which themselves incorporate design details produced by Phase 1 trade studies, and those developed for other telescoping boom programs currently under development. This CTA development activity has been crucial to ensuring that the PFC-specific technologies are not advancing beyond the state of the CTA “platform,” and have therefore allowed the EESP study to be more ambitious than what would be possible if the entire wing system had to be developed under this study. The first-generation NASA wing prototype is shown in Figure 29.

Table 12. PFC-CTA-Related Activities

Lead (partner)	Funding, Title	Time-frame	Key Activities
AD (OA)	NASA, CTA Phase 2 SBIR	6/16 - 12/17	CTA EDU, key functional aspects, less root hinge and tiedowns. Ground offloaded deployments only.
AD (OA)	AFRL, CTA Phase 2 SBIR	3/17 - 9/18	CTA EDU, including root hinge, tiedowns. Vibration and thermal system testing.
OA (MOLLC)	NASA, EESP PFC-CTA	10/16 - 4/18	Point Focus Concentrator: Pointing, thermal, system performance, etc. Subsystem prototypes & test hardware including mini blanket vibration and full PV panel LAPSS.
MOLLC (SolAero)	NASA, Phase IIE	10/16 - 4/17	25X Point Focus lens developed including lens tooling. Lens samples delivered to NASA.
MOLLC (SolAero)	NASA, CCRPP	6/17 - 3/18	Further development of 25X concentrator, mesh reinforcements, optical performance verification. Orbital ATK is an "investor" via EESP Option 1 & 2.
OA (NASA LaRC)	NASA, CIRAS (Tipping Point)	10/16 - 10/18	In-flight assembly technology demonstration program. Prototype CTA wings built to validate robotic installation and deployment.

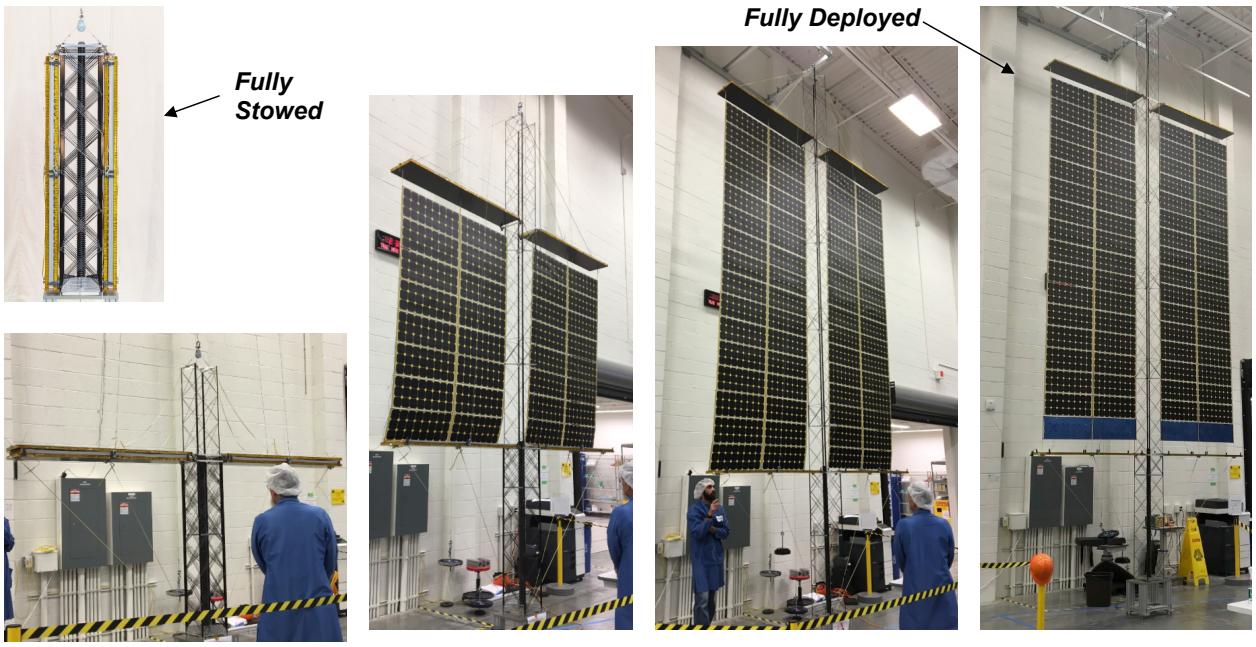

Figure 29. NASA Phase 2 SBIR CTA Wing Deployed in Cleanroom

Summary and Conclusion

Orbital ATK is pleased by the continued progress on PFC-CTA, based on our success during the Base Phase in mitigating most of the key risks associated with the preparation of this technology for space flight infusion. The structural and packaging efficiency of CTA as a 1-sun solar array has shown to be similarly enabling for a high-concentration array, providing the accurate pointing alignment and high stiffness required. The high TRL achieved rapidly during the EESP study makes breakthrough array level performance of PFC-CTA *accessible to near-term missions*, and the rapid rate at which the component elements is advancing along other fronts is further confidence that PFC-CTA technology will successfully deliver on its promised significant cost and performance benefits.

References

[1] Michael E. McEachen, et al. "Compact Telescoping Array: Advancement from Concept to Reality", 2018 AIAA Spacecraft Structures Conference, AIAA SciTech Forum, (AIAA 2018-1945) https://doi.org/10.2514/6.2018-1945

[2] M.F. Piszczor et al., "Stretched Lens Array (***SLA***) Solar Electric Propulsion (***SEP***) Space Tug: ***SLA***-***SEP*** Offers Multi-Billion-Dollar Savings Delivering Lunar Exploration Cargo," 4th World Conference on Photovoltaic Energy Conversion (WCPEC), Hawaii, May 2006.

[3] Mikulas, M. et. al., "Telescoping Solar Array Concept for Achieving High Packaging Efficiency" AIAA Spacecraft Structures Conference, January 2015.

[4] Banik, Jeremy A., "Structural Scaling Metrics for Tensioned-Blanket Space Systems" PhD diss., The University of New Mexico, Albuquerque, 2014. Banik, Jeremy A., "Structural Scaling Metrics for Tensioned-Blanket Space Systems" PhD diss., The University of New Mexico, Albuquerque, 2014.

[5] M. Bodeau, "Root-Cause of the 702 Concentrator Array Anomaly," Presentation at the 2003 Space Power Workshop, Redondo Beach, April 2003.

[6] Murphy, David M., The Scarlet Solar Array: Technology Validation and Flight Results, Deep Space 1 Technology Validation Symposium, February 8-9, 2000 at JPL, available at http://nmp-techval-reports.jpl.nasa.gov/DS1/ Scarlet_Integrated_Report.pdf

[7] Phillip Jenkins et al., "Initial Results from the ***TacSat-4*** Solar Cell Experiment," 39th IEEE Photovoltaic Specialists Conference, Tampa, June 2013.

[8] Phillip Jenkins et al., "TacSat-4 Solar Cell Experiment: Advanced Solar Cell Technologies in a High Radiation Environment," 34th IEEE Photovoltaic Specialists Conference, Philadelphia, 2009.

[9] Henry Brandhorst et al., "Test Results for a High-Voltage Multi-Junction-Cell Concentrator Array Direct-Driving an Electric Thruster," 34th IEEE Photovoltaic Specialists Conference, Philadelphia, 2009.

[10] Datasheet - DOW CORNING ® 93-500, SPACE – GRADE ENCAPSULANT

[11] Dever, Joyce A.; Yan, Li, "Vacuum Ultraviolet Radiation Effects on DC93-500 Silicone Film Studied" NASA Technical Reports Server (NTRS) 2005-01-01

[12] JPL Technical Memorandum 33-626, "Thermoelastic Analysis of Solar Cell Arrays and Their Material Properties", M. A. Salama, W. M. Rowe, R. K. Yasui, September 1, 1973.

[13] Mark O'Neill et al., "Space Photovoltaic Concentrator Using Robust Fresnel Lenses, 4-Junction Cells, Graphene Radiators, and Articulating Receivers," 43rd IEEE Photovoltaic Specialists Conference (PVSC), Portland, Oregon, June 2016.

[14] Mark O'Neill et al., "Space Photovoltaic Concentrator Using Flat Glass/Silicone Fresnel Lenses, 4-Junction IMM Cells, Graphene-Based Radiators, and Articulating Photovoltaic Receivers," 24th SPRAT Conference, Cleveland, September 2016.

[15] Murphy, D., Eskenazi, M., McEachen, M., and Spink, J., UltraFlex and MegaFlex – Advancements in Highly Scalable Solar Power, AIAA SciTech Forum, AIAA Spacecraft Structures Conference, San Diego, CA, January 2016.

[16] Jaworske, Donald A., "Hall Effect Thruster Plume Contamination and Erosion Study", NASA/TM-2000-210204, June 2000

[17] Hitoshi Kuninaka. "Space experiment on plasma interaction caused by high-voltage photovoltaic power generation", Journal of Spacecraft and Rockets, Vol. 32, No. 5 (1995), pp. 894-898. http://dx.doi.org/10.2514/3.26702

[18] Landis, Geoffry A. and Fincannon, James, "Study of Power Options for Jupiter and Outer Planet Missions," *42nd IEEE Photovoltaic Specialists Conference*, New Orleans LA, June 14-19 2015.

[18] Boca, A., Stella, P., Kerestes, C., and Sharps, P. "Solar Arrays for Low-Irradiance Low-Temperature and High Radiation Environments," NASA Extreme Environments Solar Power, Base Period Final Report, April 26, 2017.

[19] Dawson, S., Stella, P., McAlpine, W., and Smith, B. "JUNO Photovoltaic Power at Jupiter", 10th International Energy Conversion Engineering Conference, Atlanta Georgia, July 30th – August 1st, 2012.